

Title	Entanglement entropy in quantum field theory and entanglement entropic force between black holes
Author(s)	Shiba, Noburo
Citation	大阪大学, 2013, 博士論文
Version Type	VoR
URL	https://doi.org/10.18910/26157
rights	
Note	

Osaka University Knowledge Archive : OUKA

<https://ir.library.osaka-u.ac.jp/>

Osaka University

Entanglement entropy in quantum field theory and entanglement entropic force between black holes

Noburo Shiba*

*Department of Physics, Graduate School of Science,
Osaka University, Toyonaka, Osaka 560-0043, Japan*

(Dated: September 3, 2013)

Abstract

First, we study the entanglement entropy S_{AB} of a $d + 1$ dimensional massless free scalar field on two disjoint compact spatial regions A and B whose sizes are R_1 and R_2 , respectively, and the distance between them is r . The state of the massless free scalar field is the vacuum state. We consider the mutual information $S_{A;B} \equiv S_A + S_B - S_{AB}$ where S_A and S_B are the entanglement entropy on the inside region of A and B , respectively. We develop the computational method based on that of Bombelli et al and obtain the result that $S_{A;B} = \frac{1}{r^{2d-2}}G(R_1, R_2)$, when $r \gg R_1, R_2$. When A and B are spheres in $d = 2$ and 3 , we obtain explicit results $G(R_1, R_2) = 0.37R_1R_2$ for $d = 2$ and $G(R_1, R_2) = 0.26R_1^2R_2^2$ for $d = 3$ by numerical calculations.

By using the method used in the Minkowski spacetime case with some modifications, we study the entanglement entropy, S_C , of the massless free scalar field on the outside region C of two black holes A and B whose radii are R_1 and R_2 and how it depends on the distance, $r(\gg R_1, R_2)$, between two black holes. If we can consider the entanglement entropy as thermodynamic entropy, we can see the entropic force (we call this entanglement entropic force) acting on the two black holes from the r dependence of S_C . We consider the property of the entropic force.

*shiba@het.phys.sci.osaka-u.ac.jp

I. INTRODUCTION

Entanglement entropy in quantum field theory (QFT) was originally studied to explain the black hole entropy [1, 2]. Entanglement entropy is generally defined as the von Neumann entropy $S_A = -\text{Tr} \rho_A \ln \rho_A$ corresponding to the reduced density matrix ρ_A of a subsystem A . When we consider quantum field theory in $d + 1$ dimensional spacetime $\mathbb{R} \times N$, where \mathbb{R} and N denote the time direction and the d dimensional space-like manifold respectively, we define the subsystem by a d dimensional domain $A \subset N$ at fixed time $t = t_0$. (So this is also called geometric entropy.) Entanglement entropy naturally arises when we consider the black hole because we cannot obtain the information in the black hole. In fact, in the vacuum state the leading term of the entanglement entropy of A is proportional to the area of the boundary ∂A in many cases [1, 2]. This is similar to the black hole entropy, and extensive studies have been carried out [3–8].

First, we study the entanglement entropy S_{AB} of a $d + 1$ dimensional massless free scalar field on two disjoint compact spatial regions A and B whose sizes are R_1 and R_2 , respectively, and the distance between them is r . The state of the massless free scalar field is the vacuum state. In higher dimensional (more than two dimensional) QFT, it is not easy to compute the entanglement entropy for arbitrary regions even in free field theories. Entanglement entropy of two disconnected regions has been studied, see e.g. [9–11]. We studied S_{AB} in [12] analytically and in [13]. We develop the computational method based on that of Bombelli et al [1]. When $r \gg R_1, R_2$, we obtained the r dependence of S_{AB} as [12]

$$S_{AB} \approx S_A + S_B - \frac{G(R_1, R_2, a)}{r^{2d-2}}, \quad (1)$$

where a is an ultraviolet cutoff length and $G(R_1, R_2, a) = G(R_2, R_1, a) \geq 0$. We cannot obtain the explicit form of $G(R_1, R_2, a)$ analytically. When A and B are spheres in $d = 2$ and 3, we obtain explicit results for $G(R_1, R_2, a)$ by numerical calculations [13]. We obtain the result that the mutual information $S_{A:B} \equiv S_A + S_B - S_{AB}$ is independent of the ultraviolet cutoff length and $G(R_1, R_2, a)$ is proportional to the simple product of the surface areas of two spheres. (Note that we cannot determine the functional form of $G(R_1, R_2)$ only by the constraints from dimensional analysis, symmetry, and behavior in the limit $R_1 \rightarrow 0$. For example, $G(R_1, R_2) = R_1^3 R_2 + R_1 R_2^3$ is not prohibited by these constraints.) The mutual information is a quantity that measures the entanglement between two systems. (See e.g. [14]) Recently, our numerical results of the mutual information of two spheres for $d = 2$ and

$d = 3$ are checked by analytical calculation carried out by Cardy [23]. Our results agree with the results of Cardy [23] within numerical errors. In order to examine whether only the degrees of freedom on the surface of the spheres contribute to the mutual information or not, we calculate the mutual information $S_{D;E}$ of two same spherical shells D and E for $d = 3$ and the mutual information $S_{H;I}$ of two same rings H and I for $d = 2$. The internal (external) radii of the spherical shell and the ring are L_1 (L_2). The distance between the centers of the two spherical shells and that between the two rings are r . We obtain the result that $S_{D;E}$ and $S_{H;I}$ are monotone decreasing function of L_1 . Then not only the degrees of freedom on the surface of the sphere but also those on the inside region contribute to the mutual information. This result is remarkably different from that of the entanglement entropy to which the degrees of freedom on the surface of the boundary contribute mainly.

By using the method used in the Minkowski spacetime case with some modifications, we study the entanglement entropy, S_C , of the massless free scalar field on the outside region C of two black holes A and B whose radii are R_1 and R_2 and how it depends on the distance, $r(\gg R_1, R_2)$, between two black holes [12]. To a distant observer, an object falling into a black hole takes an infinite time to reach the event horizon and the outside region is isolated from the inside region if we neglect the change of the mass of the black hole. Then we are probably able to consider the entanglement entropy of quantum fields on the outside region C of two black holes A and B as thermodynamic entropy, and we can see the entropic force acting on the two black holes from the r dependence of S_C . We consider two systems X and Y , then one can show $S_X = S_Y$ in general [14] if a composite system XY is in a pure state. Then $S_C = S_{AB}$ when the state of the field on the whole space is a pure state. So we can use the method used in the Minkowski spacetime case with some modifications. We consider the case that the state of the massless free scalar field is the vacuum state which depends how to choose the time coordinate. We choose the coordinate system which covers whole space time and does not have the coordinate singularity on the horizons. We consider the property of the entropic force. We will roughly estimate the magnitude of the entropic force between two black holes by using S_{AB} in Minkowski spacetime.

We mention our assumption that we can consider the entanglement entropy of two black holes as thermodynamic entropy. The important point is that the outside region is isolated or not. To a distant observer, an object falling into a black hole takes an infinite time to reach the event horizon and the outside region is isolated from the inside region. Black holes act

as "walls" which hide inside regions but hold the entanglement between inside and outside regions. So we are probably able to consider the entanglement entropy of quantum fields on the outside region C of two black holes A and B as thermodynamic entropy. However, entanglement entropy has property which is different from that of thermodynamic entropy. So we must reconsider statistical mechanics from a fundamental level to judge whether our assumption is really correct or not.

This thesis is organized as follows. The first half is the analytical study. In Section II we review basic ideas and basic properties of entanglement entropy. In Section III we obtain the general behavior of the entanglement entropy of two disjoint regions in translational invariant vacuum in general QFT. There have been some computational methods of entanglement entropy [15–17] and the reader is urged to refer to [18–20] for reviews. Among several others, we review in Section IV the method of Bombelli et al [1] which is most straightforward and powerful enough to obtain the r dependence of S_{AB} in free scalar field theory and suitable for numerical calculations. In Section V we study S_{AB} in $d+1$ dimensional Minkowski spacetime. In this case the state of the massless free scalar field is the Minkowski vacuum state and we take the trace over the degrees of freedom residing in A and B . We develop the method of Bombelli et al and obtain the leading term of S_{AB} with respect to $1/r$. The result in this section agrees with the general behavior in Section III. This method can be used for any scalar fields in curved space time whose Lagrangian is quadratic with respect to the scalar fields (i.e higher derivative terms can exist). In Section VI we consider the black hole case. We use the method used in Section V with some modifications. We show that S_C can be expected to be the same form as that in the Minkowski spacetime case. But in the black hole case S_A and S_B depend on r , so we do not fully obtain the r dependence of S_C . In Section VII we assume that the entanglement entropy can be regarded as thermodynamic entropy, and consider the entanglement entropic force. We argue how to separate the entanglement entropic force from other force and how to cancel S_A and S_B whose r dependence are not obtained. Then we obtain the physical prediction which can be tested experimentally in principle, and discuss the possibility to measure the entanglement entropic force.

The second half is the numerical study. In Section VIII, we apply the formalism of Bombelli et al [1] to a massless free scalar field on lattices in order to calculate numerically the entanglement entropy. We improve the computational method of Bombelli et al to reduce the computational complexity. In Section IX, we numerically calculate the entanglement

entropy S_{AB} , the mutual information $S_{D;E}$, and $S_{H;I}$ in $(d + 1)$ -dimensional Minkowski spacetime for $d = 2, 3$. We roughly estimate the magnitude of the entropic force between two black holes by S_{AB} in $(3+1)$ -dimensional Minkowski spacetime. In Appendix B we obtain a formula for a finite series as a by-product of our calculation.

II. BASIC PROPERTIES OF ENTANGLEMENT ENTROPY

In this section we review basic ideas and basic properties of entanglement entropy [14, 18].

A. The definition of entanglement entropy

We consider a quantum mechanical system with many degrees of freedom such as spin chains. We divide the total system into two subsystems A and B . In the spin chain example, we just artificially cut off the chain at some point and divide the lattice points into two groups. Notice that physically we do not do anything to the system and the cutting procedure is an imaginary process. Accordingly the total Hilbert space can be written as a direct product of two spaces $H_{tot} = H_A \otimes H_B$ corresponding to those of subsystems A and B . The observer who is only accessible to the subsystem A will feel as if the total system is described by the reduced density matrix $\rho_A = tr_B \rho_{AB}$ where the trace is taken only over the Hilbert space H_B . Now we define the entanglement entropy of the subsystem A as the von Neumann entropy of the reduced density matrix ρ_A

$$S_A = -tr_A \rho_A \ln \rho_A. \quad (2)$$

Notice that $S_{AB} = 0$ does not necessarily mean $S_A = S_B = 0$. For example, we consider the case that A and B are the spin 1/2 particles and the state of total system is $|\psi\rangle = (|0\rangle |1\rangle + |1\rangle |0\rangle)/\sqrt{2}$ where $|0\rangle$ ($|1\rangle$) is the spin down (up) state. In this case $S_{AB} = 0$ and $S_A = \ln 2$ because $\rho_A = (|0\rangle \langle 0| + |1\rangle \langle 1|)/2$. The entanglement entropy measures the degree of entanglement.

When we divide the total system into three subsystems A , B , and C , we define the entanglement entropy in the same way. For example, we define the entanglement entropy of A and B as

$$S_{AB} = -tr_{AB} \rho_{AB} \ln \rho_{AB}, \quad (3)$$

where $\rho_{AB} = tr_C \rho_{ABC}$.

B. General properties

There are several useful properties which entanglement entropy enjoys generally. (See e.g. [14].) We summarize some of them for later use.

1. If a composite system AB is in a pure state, then $S_A = S_B$.
2. If $\rho_{AB} = \rho_A \otimes \rho_B$, then $S_{AB} = S_A + S_B$.
3. For any subsystem A and B , the following inequalities hold:

$$S_{AB} \leq S_A + S_B, \quad (4)$$

$$S_{AB} \geq |S_A - S_B|. \quad (5)$$

The first is the subadditivity inequality, and the second is the triangle inequality. From (4) the mutual information $S_{A:B} \equiv S_A + S_B - S_{AB}$ is always positive.

C. Entanglement entropy in QFT and area law

When we consider quantum field theory in $d + 1$ dimensional spacetime $\mathbb{R} \times N$, where \mathbb{R} and N denote the time direction and the d dimensional space-like manifold respectively, we define the subsystem by a d dimensional domain $A \subset N$ at fixed time $t = t_0$. (So this is also called geometric entropy.) In the vacuum state the leading term of the entanglement entropy of A is proportional to the area of the boundary ∂A in many cases [1, 2]. This behavior can be intuitively understood since the entanglement between A and B occurs at the boundary ∂A most strongly. However, the simple area law does not always hold. The entanglement entropy in $1 + 1$ dimensional CFT scales logarithmically with respect to the length l of A , $S_A = \frac{c}{3} \ln \frac{l}{a}$, where c is the central charge of the CFT [15].

There have been some computational methods of entanglement entropy [15–17]. We review in Section IV the method of Bombelli et al [1]. Now we mention other methods. There is a useful technique called the replica trick. In order to calculate the entanglement entropy, we first evaluate $\text{tr}_A \rho_A^n$, differentiate it with respect to n and finally take the limit $n \rightarrow 1$,

$$S_A = -\text{tr} \rho_A \log \rho_A = \lim_{n \rightarrow 1} \frac{\text{tr}_A \rho_A^n - 1}{1 - n} = -\frac{\partial}{\partial n} \text{tr}_A \rho_A^n \Big|_{n=1}. \quad (6)$$

This is the replica trick. Therefore, what we have to do is to evaluate $\text{tr}_A \rho_A^n$. The path integral representation of $\text{tr}_A \rho_A^n$ is useful for analytical studies. In [10, 11, 15], the entanglement entropy in $1 + 1$ dimensional CFT was analytically studied by using the path integral

representation. In higher dimensional (more than two dimensional) QFT, it is not easy to evaluate $tr_A \rho_A^n$. Ryu and Takayanagi [17] proposed the method to calculate entanglement entropy by using AdS/CFT correspondence. They proposed that the entanglement entropy S_A in $d + 1$ dimensional CFT can be computed from the following area law relation

$$S_A = \frac{Area(\gamma_A)}{4G_N^{(d+2)}}. \quad (7)$$

The manifold γ_A is the d -dimensional static minimal surface in AdS_{d+2} whose boundary is given by ∂A . Its area is denoted by $Area(\gamma_A)$. Also $G_N^{(d+2)}$ is the $d + 2$ dimensional Newton constant. This holographic formula reproduce the results in $1 + 1$ dimensional CFT and its validity is checked in [17, 18]. This formula is very useful in higher dimensional QFT because the calculation of $Area(\gamma_A)$ is not so difficult in higher dimensions. However, we cannot use (7) in order to calculate the entanglement entropy of two disjoint compact regions A and B in a massless free scalar field. When the separation between the two regions is large enough compared to their sizes, a disconnected surface γ_{AB}^{dis} with $Area(\gamma_{AB}^{dis}) = Area(\gamma_A) + Area(\gamma_B)$ is the minimal surface. Then, from (7) we obtain $S_{AB} = S_A + S_B$ and $S_{A;B} = S_A + S_B - S_{AB} = 0$. This result means that the correlations between A and B vanishes even if the distance between them is finite. This behaviour comes probably from the large N limit in AdS/CFT correspondence [24] and we cannot use (7) to calculate the entanglement entropy of two disjoint compact regions in a massless free scalar field.

In higher dimensional QFT, it is not easy to compute the entanglement entropy for arbitrary regions even in free field theories. Recently, Cardy develops the computational method to calculate the mutual information of two disjoint compact regions in the limit when the separation between them is much greater than their sizes [23]. This method is based on the path integral representation of $tr_{AB} \rho_{AB}^n$. He calculated the mutual information of two spheres A and B for $d = 2$ and $d = 3$ [23]. The results are $S_{A;B} = \frac{1}{3}R_1R_2/r^2$ for $d = 2$ and $S_{A;B} = \frac{4}{15}R_1^2R_2^2/r^4$ for $d = 3$. ($4/15 = 0.266\dots$) On the other hand, our numerical results are $S_{A;B} = 0.37R_1R_2/r^2$ for $d = 2$ and $S_{A;B} = 0.26R_1^2R_2^2/r^4$ for $d = 3$. The corrections to the leading terms of $S_{A;B}$ with respect to $1/r$ are more important in $d = 2$ than $d = 3$ which may account for the above discrepancy [23].

III. GENERAL BEHAVIOR

We consider entanglement entropy of two disjoint regions (A and B) in translational invariant vacuum in general QFT in $d+1$ dimensional spacetime ($d \geq 2$). We will show that S_C reaches its maximum value when $r \rightarrow \infty$, where C is the outside region of A and B .

Because of translational invariance, S_A and S_B are independent of their positions, so, $\frac{\partial S_A}{\partial r} = 0$ and $\frac{\partial S_B}{\partial r} = 0$. And the total system is in a pure state, so we have $S_C = S_{AB}$. Moreover, in the vacuum state, $\lim_{r \rightarrow \infty} \rho_{AB} = \rho_A \otimes \rho_B$ because of the cluster decomposition principle [25]. So the general property 2 suggests

$$\lim_{r \rightarrow \infty} S_C(r) = S_A + S_B. \quad (8)$$

We apply (4) and (5) to this system, then we obtain

$$|S_A - S_B| \leq S_C(r) \leq S_A + S_B. \quad (9)$$

Eqs. (8) and (9) show that S_C (as a function of r) reaches its maximum value when $r \rightarrow \infty$.

IV. HOW TO COMPUTE ENTANGLEMENT ENTROPY

In this section we review the computational method developed by Bombelli et al [1].

A. Entanglement entropy of a collection of coupled harmonic oscillators

As a model amenable to unambiguous calculation we deal with the scalar field on \mathbb{R}^d as a collection of coupled oscillators on a lattice of space points, labeled by capital Latin indices, the displacement at each point giving the value of the scalar field there. In this case the Lagrangian can be given by

$$L = \frac{1}{2} G_{MN} \dot{q}^M \dot{q}^N - \frac{1}{2} V_{MN} q^M q^N, \quad (10)$$

where q^M gives the displacement of the M th oscillator and \dot{q}^M its generalized velocity. The symmetric matrix G_{MN} is positive definite and therefore invertible; i.e., there exists the inverse matrix G^{MN} such that

$$G^{MP} G_{PN} = \delta^M_N. \quad (11)$$

The matrix V_{MN} is also symmetric and positive definite. The matrices G_{MN} and V_{MN} are independent of q^M and \dot{q}^M . Introducing the conjugate momentum to q^M ,

$$P_M = G_{MN}\dot{q}^N, \quad (12)$$

we can write the Hamiltonian for our system as

$$H = \frac{1}{2}G^{MN}P_MP_N + \frac{1}{2}V_{MN}q^Mq^N. \quad (13)$$

Next, consider the positive definite symmetric matrix W_{MN} defined by

$$W_{MA}G^{AB}W_{BN} = V_{MN}. \quad (14)$$

In this sense the matrix W is the "square root" of V in the scalar product with G .

Now consider a region Ω in \mathbb{R}^d . The oscillators in this region will be specified by Greek letters, and those in the complement of Ω , Ω^c , will be specified by lowercase Latin letters.

We will use the following notation

$$W_{AB} = \begin{pmatrix} W_{ab} & W_{a\beta} \\ W_{\alpha b} & W_{\alpha\beta} \end{pmatrix} \equiv \begin{pmatrix} A & B \\ B^T & C \end{pmatrix} \quad W^{AB} = \begin{pmatrix} W^{ab} & W^{a\beta} \\ W^{\alpha b} & W^{\alpha\beta} \end{pmatrix} \equiv \begin{pmatrix} D & E \\ E^T & F \end{pmatrix}, \quad (15)$$

where W^{AB} is the inverse matrix of W_{AB} (W^{AB} is *not* obtained by raising indices with G^{AB}).

So we have

$$\begin{pmatrix} 1 & 0 \\ 0 & 1 \end{pmatrix} = \begin{pmatrix} A & B \\ B^T & C \end{pmatrix} \begin{pmatrix} D & E \\ E^T & F \end{pmatrix} = \begin{pmatrix} AD + BE^T & AE + BF \\ B^TD + CE^T & B^TE + CF \end{pmatrix}. \quad (16)$$

If the information on the displacement of the oscillators in Ω is considered as unavailable, we can obtain a reduced density matrix ρ_{red} for Ω^c , integrating out over $q^\alpha \in \mathbb{R}$ for each of the oscillators in the region Ω , and then we have

$$\rho_{red}(q^a, q^b) = \int \prod_{\alpha} dq^{\alpha} \rho(q^a, q^{\alpha}, q^b, q^{\alpha}), \quad (17)$$

where ρ is a density matrix of the total system.

We can obtain the density matrix for the ground state by the standard method, and it is a Gaussian density matrix. Then, ρ_{red} is obtained by a Gaussian integral, and it is also a Gaussian density matrix. The entanglement entropy $S = -tr \rho_{red} \ln \rho_{red}$ is given by [1]

$$S = \sum_n f(\lambda_n), \quad (18)$$

$$f(\lambda) \equiv \ln\left(\frac{1}{2}\lambda^{1/2}\right) + (1 + \lambda)^{1/2} \ln[(1 + \lambda^{-1})^{1/2} + \lambda^{-1/2}], \quad (19)$$

where λ_n are the eigenvalues of the matrix

$$\Lambda^a_b = -W^{a\alpha}W_{\alpha b} = -(EB^T)^a_b = (DA)^a_b - \delta^a_b. \quad (20)$$

In the last equality we have used (16). The last expression in (20) is useful for numerical calculations when Ω^c is smaller than Ω , because the indices of A and D take over only the space points on Ω^c and the matrix sizes of A and D are smaller than those of B and E . It can be shown that all of λ_n are non-negative as follows. From (16) we have

$$A\Lambda = -AEB^T = BFB^T. \quad (21)$$

It is easy to show that A, C, D and F are positive definite matrices when W and W^{-1} are positive definite matrices. Then $A\Lambda$ is a positive semidefinite matrix as can be seen from (21). So all eigenvalues of Λ are non-negative. After all, we can obtain the entanglement entropy by solving the eigenvalue problem of Λ .

B. The continuum limit

Next, we apply the above formalism to a massless free scalar field in $(d+1)$ dimensional Minkowski spacetime. We take the continuum limit in the above formalism. In this case the Lagrangian is given by

$$L = \int d^d x \frac{1}{2} [\dot{\phi}^2 - (\nabla\phi)^2]. \quad (22)$$

Then the potential term becomes

$$\frac{1}{2} V_{AB} q^A q^B \rightarrow \int d^d x \frac{1}{2} [(\nabla\phi)^2]. \quad (23)$$

The matrices V, W and W^{-1} are given in the momentum representation by,

$$V(x, y) = \int \frac{d^d k}{(2\pi)^d} (k^2) e^{ik \cdot (x-y)} \quad (24)$$

$$W(x, y) = \int \frac{d^d k}{(2\pi)^d} (k^2)^{1/2} e^{ik \cdot (x-y)} \quad (25)$$

$$W^{-1}(x, y) = \int \frac{d^d k}{(2\pi)^d} (k^2)^{-1/2} e^{ik \cdot (x-y)} \quad (26)$$

From (20), the matrix Λ is obtained as a sum over the oscillators in the region Ω ,

$$\Lambda(x, y) = - \int_{\Omega} d^d z W^{-1}(x, z) W(z, y). \quad (27)$$

We now have to solve the eigenvalue equation

$$\int_{\Omega^c} d^d y \Lambda(x, y) f(y) = \lambda f(x), \quad (28)$$

where Ω^c is the complementary set of Ω , and then we use the eigenvalues in the expression for the entropy (18).

V. ENTANGLEMENT ENTROPY OF TWO DISJOINT REGIONS IN A MASSLESS FREE SCALAR FIELD IN $d+1$ DIMENSIONAL MINKOWSKI SPACETIME

We consider two spheres A and B whose radii are R_1 and R_2 , and define the outside region as C . (See Fig 1.) We derive the $r(\gg R_1, R_2)$ dependence of $S_C(r, R_1, R_2)$ by using the formalism of the preceding section. (In the later analysis we do not use the shapes of A and B , so all analysis in this section holds for A and B which have arbitrary shapes. In this case R_1 and R_2 are the characteristic sizes of A and B .)

We consider $S_{AB}(r, R_1, R_2)$ because $S_C = S_{AB}$ in a pure state and the r dependence of S_{AB} is clearer than that of S_C in the calculation. In this case the region Ω is C .

We obtain the r dependence of S_{AB} by following three steps:

(1) We obtain the r dependence of Λ by using the $\|x - y\|$ dependences of $W(x, y)$ and $W^{-1}(x, y)$. We decompose Λ into the non-perturbative part and the perturbative part as $\Lambda = \Lambda^0 + \delta\Lambda$, where $\Lambda^0 \equiv \lim_{r \rightarrow \infty} \Lambda$.

(2) We obtain $\lambda_m(r)$ which are the eigenvalues of Λ by perturbation theory. This is almost similar to the time-independent perturbation theory in quantum mechanics in the presence of degeneracy. We can regard Λ as Hamiltonian. Note that Λ is *not* a symmetric matrix. So we must slightly modify the perturbation theory in quantum mechanics.

(3) In Step (2), we had $\lambda_m(r)$ as $\lambda_m(r) = \lambda_m^0 + \delta\lambda_m(r)$, where λ_m^0 are the eigenvalues of Λ^0 . We substitute these $\lambda_m(r)$ into (19), then we obtain $S_{AB}(r, R_1, R_2)$.

First we examine the $\|x - y\|$ dependences of $W(x, y)$ and $W^{-1}(x, y)$. Generally entanglement entropy has UV divergence as discussed in [1]. So we use a momentum cutoff l^{-1} in integrals (24)-(26), though these integrals are well defined as Fourier transforms of distributions. (The other regularization methods are discussed in [1].) When $d \geq 2$ and $l/\|x - y\| \rightarrow 0$, $W(x, y)$ and $W^{-1}(x, y)$ are

$$W(x, y) = \frac{A_d}{\|x - y\|^{d+1}}, \quad W^{-1}(x, y) = \frac{B_d}{\|x - y\|^{d-1}}, \quad A_d, B_d \in \mathbb{R} \quad (29)$$

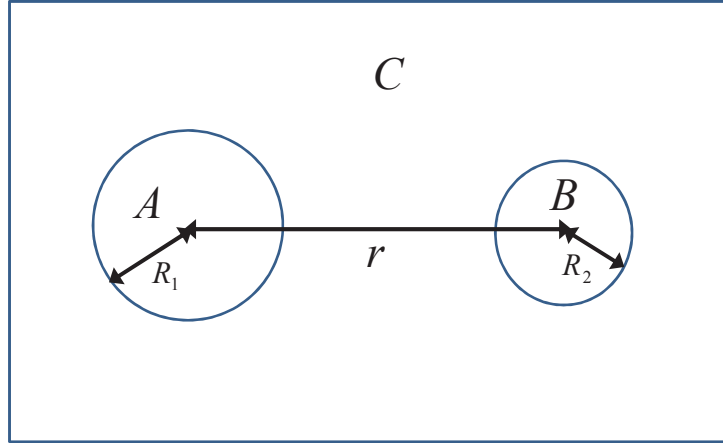


FIG. 1. Two spheres A and B , and the outside region C .

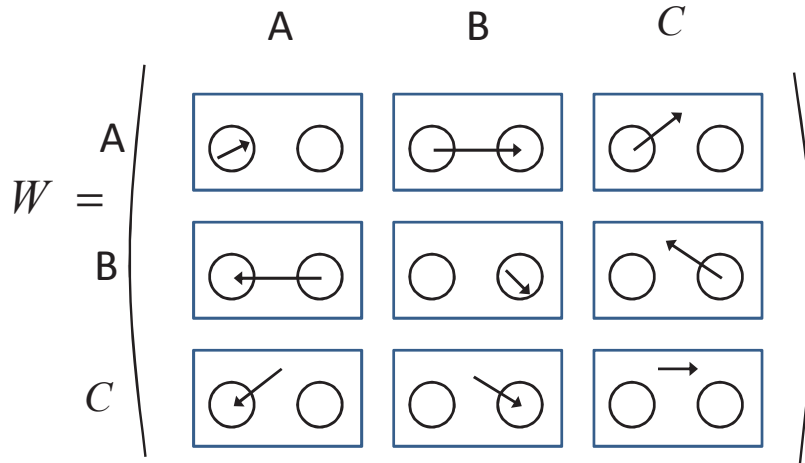


FIG. 2. The matrix elements of W . The lines denote the matrix elements $W(x, y)$ in (29). An initial point and an end point of an arrow denote a row and a column respectively. We can obtain products of matrices by connecting arrows and integrating joint points on regions where the joint points exist. Instead of solid lines we use dotted lines for W^{-1} .

where A_d and B_d are nonzero dimensionless constants (see Appendix A). We *cannot* obtain (29) by only using a dimensional analysis because $l/\|x - y\|$ is dimensionless. Indeed $V(x, y) \rightarrow 0$ when $l/\|x - y\| \rightarrow 0$, i.e. $V(x, y)$ is zero when $\|x - y\|$ is finite. On the other hand W and W^{-1} have nonzero value for $\|x - y\| > 0$ because they are kernels of integral operators of nonlocal interaction (i.e Fourier transformations of $(\sqrt{k^2})^{\pm 1}$). In Appendix A we explicitly show that W and W^{-1} have nonzero value for $\|x - y\| > 0$ and Eq. (29) holds.

Next, we obtain the r dependence of Λ by using (29). We represent the matrix elements

$$\Lambda = - \left(\begin{array}{c} \boxed{\begin{array}{c} \circ \xrightarrow{\text{dotted}} \circ \\ \circ \xleftarrow{\text{dotted}} \circ \end{array}} \\ \boxed{\begin{array}{c} \circ \xrightarrow{\text{dotted}} \circ \\ \circ \xleftarrow{\text{dotted}} \circ \end{array}} \end{array} \right) \left(\begin{array}{cc} \boxed{\begin{array}{c} \circ \xrightarrow{\text{solid}} \circ \\ \circ \xleftarrow{\text{solid}} \circ \end{array}} & \boxed{\begin{array}{c} \circ \xrightarrow{\text{solid}} \circ \\ \circ \xleftarrow{\text{solid}} \circ \end{array}} \end{array} \right)$$

$$= - \left(\begin{array}{cc} \boxed{\begin{array}{c} \circ \xrightarrow{\text{solid}} \circ \\ \circ \xleftarrow{\text{dotted}} \circ \end{array}} & \boxed{\begin{array}{c} \circ \xrightarrow{\text{dotted}} \circ \\ \circ \xleftarrow{\text{solid}} \circ \end{array}} \\ \boxed{\begin{array}{c} \circ \xrightarrow{\text{dotted}} \circ \\ \circ \xleftarrow{\text{solid}} \circ \end{array}} & \boxed{\begin{array}{c} \circ \xrightarrow{\text{solid}} \circ \\ \circ \xleftarrow{\text{dotted}} \circ \end{array}} \end{array} \right)$$

FIG. 3. The diagrammatic calculation of Λ in (30).

$$\Lambda = \left(\begin{array}{cc} - \boxed{\begin{array}{c} \circ \xrightarrow{\text{solid}} \circ \\ \circ \xleftarrow{\text{dotted}} \circ \end{array}} & \boxed{\begin{array}{c} \circ \xrightarrow{\text{dotted}} \circ \\ \circ \xleftarrow{\text{solid}} \circ \end{array}} + \boxed{\begin{array}{c} \circ \xrightarrow{\text{solid}} \circ \\ \circ \xleftarrow{\text{dotted}} \circ \end{array}} \\ \boxed{\begin{array}{c} \circ \xrightarrow{\text{dotted}} \circ \\ \circ \xleftarrow{\text{solid}} \circ \end{array}} + \boxed{\begin{array}{c} \circ \xrightarrow{\text{solid}} \circ \\ \circ \xleftarrow{\text{dotted}} \circ \end{array}} & - \boxed{\begin{array}{c} \circ \xrightarrow{\text{solid}} \circ \\ \circ \xleftarrow{\text{dotted}} \circ \end{array}} \end{array} \right)$$

$$\boxed{\begin{array}{c} \circ \xrightarrow{\text{dotted}} \circ \\ \circ \xleftarrow{\text{solid}} \circ \end{array}} + \boxed{\begin{array}{c} \circ \xrightarrow{\text{dotted}} \circ \\ \circ \xleftarrow{\text{solid}} \circ \end{array}} + \boxed{\begin{array}{c} \circ \xrightarrow{\text{solid}} \circ \\ \circ \xleftarrow{\text{dotted}} \circ \end{array}} = \mathbf{0}$$

FIG. 4. The diagrammatic representations of Λ in (32) and the identity in (31).

$$\delta\Lambda_1 \equiv \left(\begin{array}{cc} \mathbf{0} & \boxed{\begin{array}{c} \circ \xrightarrow{\text{dotted}} \circ \\ \circ \xleftarrow{\text{solid}} \circ \end{array}} \\ \boxed{\begin{array}{c} \circ \xrightarrow{\text{solid}} \circ \\ \circ \xleftarrow{\text{dotted}} \circ \end{array}} & \mathbf{0} \end{array} \right) \quad \delta\Lambda_2 \equiv \left(\begin{array}{cc} \mathbf{0} & \boxed{\begin{array}{c} \circ \xrightarrow{\text{solid}} \circ \\ \circ \xleftarrow{\text{dotted}} \circ \end{array}} \\ \boxed{\begin{array}{c} \circ \xrightarrow{\text{dotted}} \circ \\ \circ \xleftarrow{\text{solid}} \circ \end{array}} & \mathbf{0} \end{array} \right)$$

$$\Lambda_D \equiv \left(\begin{array}{cc} - \boxed{\begin{array}{c} \circ \xrightarrow{\text{solid}} \circ \\ \circ \xleftarrow{\text{dotted}} \circ \end{array}} & \mathbf{0} \\ \mathbf{0} & - \boxed{\begin{array}{c} \circ \xrightarrow{\text{solid}} \circ \\ \circ \xleftarrow{\text{dotted}} \circ \end{array}} \end{array} \right)$$

$$\Lambda = \Lambda_D + \delta\Lambda_1 + \delta\Lambda_2$$

FIG. 5. The diagrammatic representations of $\delta\Lambda_1$, $\delta\Lambda_2$ and Λ_D .

$$\begin{aligned}
\Lambda^0 &= - \begin{pmatrix} \boxed{\text{diag}} & \mathbf{0} \\ \mathbf{0} & \boxed{\text{diag}} \end{pmatrix} \equiv \begin{pmatrix} \Lambda^{01} & \mathbf{0} \\ \mathbf{0} & \Lambda^{02} \end{pmatrix} \\
A^0 &= - \begin{pmatrix} \boxed{\text{diag}} & \mathbf{0} \\ \mathbf{0} & \boxed{\text{diag}} \end{pmatrix} \\
A^0 \delta \Lambda_1 &= \begin{pmatrix} \mathbf{0} & \boxed{\text{diag}} \\ \boxed{\text{diag}} & \mathbf{0} \end{pmatrix}
\end{aligned}$$

FIG. 6. The diagrammatic representations of Λ^0 , A^0 and $A^0 \delta \Lambda_1$.

$$\begin{aligned}
\delta \Lambda_D &= \Lambda_D - \Lambda_0 \\
&= \begin{pmatrix} \boxed{\text{diag}} - \boxed{\text{diag}} & \mathbf{0} \\ \mathbf{0} & \boxed{\text{diag}} - \boxed{\text{diag}} \end{pmatrix} \\
&= \begin{pmatrix} \boxed{\text{diag}} & \mathbf{0} \\ \mathbf{0} & \boxed{\text{diag}} \end{pmatrix}
\end{aligned}$$

FIG. 7. The diagrammatic calculation of $\delta \Lambda_D$ in (41).

of $W(W^{-1})$ diagrammatically in Fig 2. Instead of solid lines we use dotted lines for W^{-1} . The lines denote the matrix elements $W(x, y)$ (or $W^{-1}(x, y)$) in (29). An initial point and an end point of an arrow denote a row and a column respectively. We can obtain products of matrices by connecting arrows and integrating joint points on regions where the joint points exist. We label coordinates in A, B and C as x_a, x_b and x_c . Then, from Fig 3 we obtain $\Lambda = -EB^T$ as

$$\begin{aligned}
\Lambda &= \begin{pmatrix} \Lambda(x_a, y_a) & \Lambda(x_a, y_b) \\ \Lambda(x_b, y_a) & \Lambda(x_b, y_b) \end{pmatrix} = - \begin{pmatrix} W^{-1}(x_a, z_c) \\ W^{-1}(x_b, z_c) \end{pmatrix} \begin{pmatrix} W(z_c, y_a) & W(z_c, y_b) \end{pmatrix} \\
&= - \begin{pmatrix} \int_C d^d z_c W^{-1}(x_a, z_c) W(z_c, y_a) & \int_C d^d z_c W^{-1}(x_a, z_c) W(z_c, y_b) \\ \int_C d^d z_c W^{-1}(x_b, z_c) W(z_c, y_a) & \int_C d^d z_c W^{-1}(x_b, z_c) W(z_c, y_b) \end{pmatrix}.
\end{aligned} \tag{30}$$

To make the r dependence of the non-diagonal elements of Λ clear, we use the following identity,

$$\int_{A+B+C} d^d z W^{-1}(x_a, z) W(z, y_b) = \delta(x_a - y_b) = 0. \quad (31)$$

We represent this identity diagrammatically in Fig 4. From (30) and (31) we obtain (see Fig 4)

$$\begin{aligned} \Lambda(x_a, y_b) &= \int_A d^d z_a W^{-1}(x_a, z_a) W(z_a, y_b) + \int_B d^d z_b W^{-1}(x_a, z_b) W(z_b, y_b) \\ \Lambda(x_b, y_a) &= \int_A d^d z_a W^{-1}(x_b, z_a) W(z_a, y_a) + \int_B d^d z_b W^{-1}(x_b, z_b) W(z_b, y_a). \end{aligned} \quad (32)$$

Note that from (29) $W(x, y)$ and $W^{-1}(x, y)$ have the different $\|x - y\|$ dependence. So, from (30) and (32) we decompose Λ as

$$\Lambda = \Lambda_D + \delta\Lambda_1 + \delta\Lambda_2 \quad (33)$$

where we define (see Fig 5)

$$\Lambda_D \equiv \begin{pmatrix} \Lambda(x_a, y_a) & 0 \\ 0 & \Lambda(x_b, y_b) \end{pmatrix}, \quad (34)$$

$$\delta\Lambda_1 \equiv \begin{pmatrix} 0 & \int_B d^d z_b W^{-1}(x_a, z_b) W(z_b, y_b) \\ \int_A d^d z_a W^{-1}(x_b, z_a) W(z_a, y_a) & 0 \end{pmatrix}, \quad (35)$$

$$\delta\Lambda_2 \equiv \begin{pmatrix} 0 & \int_A d^d z_a W^{-1}(x_a, z_a) W(z_a, y_b) \\ \int_B d^d z_b W^{-1}(x_b, z_b) W(z_b, y_a) & 0 \end{pmatrix}. \quad (36)$$

We approximate $W(x_a, y_b) \approx \frac{A_d}{r^{d+1}}$ and $W^{-1}(x_a, y_b) \approx \frac{B_d}{r^{d-1}}$ because $r \gg R_1, R_2$. Then we have

$$\delta\Lambda_1 \approx \frac{B_d}{r^{d-1}} \begin{pmatrix} 0 & \int_B d^d z_b W(z_b, y_b) \\ \int_A d^d z_a W(z_a, y_a) & 0 \end{pmatrix}, \quad (37)$$

$$\delta\Lambda_2 \approx \frac{A_d}{r^{d+1}} \begin{pmatrix} 0 & \int_A d^d z_a W^{-1}(x_a, z_a) \\ \int_B d^d z_b W^{-1}(x_b, z_b) & 0 \end{pmatrix}. \quad (38)$$

Next we consider the non-perturbative part $\Lambda^0 = \lim_{r \rightarrow \infty} \Lambda$. From (37) and (38) we can see that $\delta\Lambda_1$ and $\delta\Lambda_2$ become 0 when $r \rightarrow \infty$. Note that the integral region of the integral in $\Lambda(x_a, y_a)$ ($\Lambda(x_b, y_b)$) become $A^c \equiv \mathbb{R}^d - A$ ($B^c \equiv \mathbb{R}^d - B$) when $r \rightarrow \infty$, then we obtain

(see Fig 6)

$$\Lambda^0 = - \begin{pmatrix} \int_{A^c} d^d z W^{-1}(x_a, z) W(z, y_a) & 0 \\ 0 & \int_{B^c} d^d z W^{-1}(x_b, z) W(z, y_b) \end{pmatrix}. \quad (39)$$

From (39) we rewrite (33) as follows,

$$\Lambda = \Lambda^0 + \delta\Lambda_1 + \delta\Lambda_2 + \delta\Lambda_D, \quad (40)$$

where we define (see Fig 7)

$$\delta\Lambda_D \equiv \Lambda_D - \Lambda^0 = \begin{pmatrix} \int_B d^d z_b W^{-1}(x_a, z_b) W(z_b, y_a) & 0 \\ 0 & \int_A d^d z_a W^{-1}(x_b, z_a) W(z_a, y_b) \end{pmatrix}. \quad (41)$$

We use the same approximation as we used in (37) and (38), then we obtain

$$\delta\Lambda_D \approx \frac{A_d B_d}{r^{2d}} \begin{pmatrix} \int_B d^d z_b & 0 \\ 0 & \int_A d^d z_a \end{pmatrix}. \quad (42)$$

When we perform the perturbative calculation to obtain $\lambda_m(r)$ which is the eigenvalues of Λ , from (37), (38), (40) and (42) we can neglect $\delta\Lambda_D$ because it is higher order than $\delta\Lambda_1$ and $\delta\Lambda_2$ with respect to $1/r$. And we can neglect $\delta\Lambda_2$ because its nonzero matrix elements are in the same position as $\delta\Lambda_1$ and $\delta\Lambda_2$ is higher order than $\delta\Lambda_1$ with respect to $1/r$.

Because Λ is not a symmetric matrix, in the later perturbative calculation we need $A^0 \delta\Lambda_1$ where A^0 is defined as (see Fig 6)

$$A^0 \equiv \lim_{r \rightarrow \infty} A = \begin{pmatrix} W(x_a, y_a) & 0 \\ 0 & W(x_b, y_b) \end{pmatrix}. \quad (43)$$

From (35), (37) and (43) we obtain (see Fig 6)

$$\begin{aligned} A^0 \delta\Lambda_1 &= \begin{pmatrix} 0 & \int_A d^d z_a \int_B d^d z_b W(x_a, z_a) W^{-1}(z_a, z_b) W(z_b, y_b) \\ \int_B d^d z_b \int_A d^d z_a W(x_b, z_b) W^{-1}(z_b, z_a) W(z_a, y_a) & 0 \end{pmatrix} \\ &\approx \frac{B_d}{r^{d-1}} \begin{pmatrix} 0 & \int_A d^d z_a W(x_a, z_a) \int_B d^d z_b W(z_b, y_b) \\ \int_B d^d z_b W(x_b, z_b) \int_A d^d z_a W(z_a, y_a) & 0 \end{pmatrix}. \end{aligned} \quad (44)$$

We have finished the first step.

Next, we calculate $\lambda_m(r)$ by perturbation theory. This is almost similar to the time-independent perturbation theory with degeneracy of quantum mechanics. The only difference is that Λ is *not* a symmetric matrix and $A\Lambda$ is a symmetric matrix.

We can approximate $\Lambda \approx \Lambda^0 + \delta\Lambda_1$ and regard $\delta\Lambda_1$ as the perturbative part. Then, from (37) we expand $\lambda_m(r)$ with respect to $1/r^{d-1}$. We expand λ_m around $\lambda_m^0 \equiv \lambda_m(r = \infty)$,

$$\lambda_m = \lambda_m^0 + \delta\lambda_m^1 + \delta\lambda_m^2, \quad (45)$$

where $\delta\lambda_m^1$ and $\delta\lambda_m^2$ are the first and the second order perturbations.

Next we substitute (45) into (19),

$$\begin{aligned} S_{AB}(r, R_1, R_2) &= \sum_m f(\lambda_m) \\ &= S_A(R_1) + S_B(R_2) + \sum_m \left[\delta\lambda_m \frac{df}{d\lambda_m} \Big|_{\lambda_m=\lambda_m^0} + \frac{1}{2}(\delta\lambda_m)^2 \frac{d^2f}{d\lambda_m^2} \Big|_{\lambda_m=\lambda_m^0} \right], \end{aligned} \quad (46)$$

where $\delta\lambda_m \equiv \delta\lambda_m^1 + \delta\lambda_m^2$. We will show that the first order perturbation in (46) (i.e. $\sum_m \delta\lambda_m^1 \frac{df}{d\lambda_m} \Big|_{\lambda_m=\lambda_m^0}$) is zero, so we must calculate the second order perturbations.

We label the λ_m^0 's as $\lambda_m^0 > \lambda_n^0$ when $m > n$. And we define the eigenvectors of Λ^0 ,

$$f_{m1\alpha}^0 = \begin{pmatrix} f_{m1\alpha}^0(x_a) \\ 0 \end{pmatrix}, f_{n2\beta}^0 = \begin{pmatrix} 0 \\ f_{n2\beta}^0(x_b) \end{pmatrix}, \Lambda^0 f_{m1\alpha}^0 = \lambda_m^0 f_{m1\alpha}^0, \Lambda^0 f_{n2\beta}^0 = \lambda_n^0 f_{n2\beta}^0, \quad (47)$$

where $\alpha = 1, \dots, M_m$ and $\beta = 1, \dots, N_n$ are the labels of the degeneracy. And we normalize $f_{mi\alpha}^0$ ($i = 1, 2$) as follow,

$$f_{mi\alpha}^{0T} A^0 f_{nj\beta}^0 = \delta_{mn} \delta_{ij} \delta_{\alpha\beta}. \quad (48)$$

This normalization is always possible because A^0 is a positive definite symmetric matrix. For general R_1 and R_2 , Λ^{01} and Λ^{02} have different eigenvalues, so there are two groups of λ_m^0 ; one is the group of the common eigenvalues of Λ^{01} and Λ^{02} , the other is not. We will see that $\delta\lambda_m^1$ of the latter group are zero. We expand $f_{m\gamma}$ which is the eigenvector of Λ in the following way,

$$f_{m\gamma} = \sum_{\alpha} a_{\gamma\alpha} f_{m1\alpha}^0 + \sum_{\beta} b_{\gamma\beta} f_{m2\beta}^0 + f_{m\gamma}^1 + f_{m\gamma}^2 \equiv \xi_{m\gamma}^0 + f_{m\gamma}^1 + f_{m\gamma}^2 \quad (49)$$

where $f_{m\gamma}^1$ and $f_{m\gamma}^2$ are the first and the second order perturbations. Note that when λ_m^0 is an eigenvalue of Λ^{01} (Λ^{02}) and is not an eigenvalue of Λ^{02} (Λ^{01}), then the coefficients $b_{\gamma\beta}$

$(a_{\gamma\alpha})$ are zero ; because the zeroth order eigenvectors $f_{m2\beta}^0$ ($f_{m1\alpha}^0$) do not exist. So either the coefficients $a_{\gamma\alpha}$ or $b_{\gamma\beta}$ are zero when λ_m^0 is not a common eigenvalue of Λ^{01} and Λ^{02} . We substitute (49) into the eigenvalue equation (we approximate $\Lambda \approx \Lambda^0 + \delta\Lambda_1$), then we have

$$(\Lambda^0 + \delta\Lambda_1)f_{m\gamma} = (\lambda_m^0 + \delta\lambda_{m\gamma}^1 + \delta\lambda_{m\gamma}^2)f_{m\gamma}. \quad (50)$$

We obtain equations of the first and the second order perturbation.

$$\Lambda^0 f_{m\gamma}^1 + \delta\Lambda_1 \xi_{m\gamma}^0 = \lambda_m^0 f_{m\gamma}^1 + \delta\lambda_{m\gamma}^1 \xi_{m\gamma}^0, \quad (51)$$

$$\Lambda^0 f_{m\gamma}^2 + \delta\Lambda_1 f_{m\gamma}^1 = \lambda_m^0 f_{m\gamma}^2 + \delta\lambda_{m\gamma}^1 f_{m\gamma}^1 + \delta\lambda_{m\gamma}^2 \xi_{m\gamma}^0. \quad (52)$$

We multiply (51) by $f_{mj\gamma'}^{0T} A^0$ from the left . The first term of the left hand side of (51) cancel the first term of the right hand side of (51) because $A^0 \Lambda^0$ is a symmetric matrix, then we obtain

$$\sum_{\alpha} a_{\gamma\alpha} V_{m\gamma'm\alpha}^{j1} + \sum_{\beta} b_{\gamma\beta} V_{m\gamma'm\beta}^{j2} = \delta\lambda_{m\gamma}^1 (a_{\gamma\gamma'} \delta^{j1} + b_{\gamma\gamma'} \delta^{j2}), \quad (53)$$

where

$$V_{m\alpha n\beta}^{ij} \equiv f_{mi\alpha}^{0T} A^0 \delta\Lambda_1 f_{nj\beta}^0. \quad (54)$$

From (44) we obtain $V_{m\alpha n\beta}^{11} = V_{m\alpha n\beta}^{22} = 0$ and

$$\begin{aligned} V_{m\alpha n\beta}^{12} &= \begin{pmatrix} f_{m1\alpha}^0(x_a) & 0 \end{pmatrix} \begin{pmatrix} A^0 \delta\Lambda_1(x_a, y_a) & A^0 \delta\Lambda_1(x_a, y_b) \\ A^0 \delta\Lambda_1(x_b, y_a) & A^0 \delta\Lambda_1(x_b, y_b) \end{pmatrix} \begin{pmatrix} 0 \\ f_{n2\beta}^0(y_b) \end{pmatrix} \\ &= \frac{B_d}{r^{d-1}} \int_A d^d x_a \int_A d^d z_a W(x_a, z_a) f_{m1\alpha}^0(x_a) \int_B d^d y_b \int_B d^d z_b W(y_b, z_b) f_{n2\beta}^0(y_b) \equiv \frac{B_d}{r^{d-1}} C_{m\alpha n\beta} \end{aligned} \quad (55)$$

and $V_{m\alpha n\beta}^{12} = V_{n\beta m\alpha}^{21}$. We define an $M_m \times N_n$ matrix C_{mn} as $(C_{mn})_{\alpha\beta} = C_{m\alpha n\beta}$ and write (53) as follows,

$$\frac{B_d}{r^{d-1}} \begin{pmatrix} 0 & C_{mm} \\ C_{mm}^T & 0 \end{pmatrix} \begin{pmatrix} \mathbf{a}_{\gamma} \\ \mathbf{b}_{\gamma} \end{pmatrix} = \delta\lambda_{m\gamma}^1 \begin{pmatrix} \mathbf{a}_{\gamma} \\ \mathbf{b}_{\gamma} \end{pmatrix} \quad (56)$$

where $(\mathbf{a}_{\gamma})_{\alpha} = a_{\gamma\alpha}$ and $(\mathbf{b}_{\gamma})_{\beta} = b_{\gamma\beta}$. From (56), if λ_m^0 is not a common eigenvalue of Λ^{01} and Λ^{02} , $\delta\lambda_{m\gamma}^1$ is zero; because either $a_{\gamma\alpha}$ or $b_{\gamma\beta}$ are zero when λ_m^0 is not a common eigenvalue of Λ^{01} and Λ^{02} . We first consider the case that $M_m \geq N_n$. In this case we obtain the following

eigenvalue equation [26].

$$\begin{aligned} \det \begin{vmatrix} x1_{M_m \times M_m} & -C_{mm} \\ -C_{mm}^T & x1_{N_m \times N_m} \end{vmatrix} &= \det(x1_{M_m \times M_m}) \det(x1_{N_m \times N_m} - x^{-1}C_{mm}^T C_{mm}) \\ &= x^{M_m - N_m} \det(x^2 1_{N_m \times N_m} - C_{mm}^T C_{mm}) = 0. \end{aligned} \quad (57)$$

We define the eigenvalues of $C_{mm}^T C_{mm}$ as $c_{m\alpha}$ ($\alpha = 1, \dots, M_m$). $C_{mm}^T C_{mm}$ is a positive semidefinite matrix because C_{mm} is a real matrix, so $c_{m\alpha} \geq 0$. Then we obtain $\delta\lambda_{m\gamma}^1$ from (56) and (57) .

$$\delta\lambda_{m\gamma}^1 = \begin{cases} 0 \\ \pm \frac{B_d}{r^{d-1}} \sqrt{c_{m\alpha}} \quad (\alpha = 1, \dots, M_m) \end{cases}. \quad (58)$$

When $M_m < N_m$, we can obtain $\delta\lambda_{m\gamma}^1$ in the same way. We define the eigenvalues of $C_{mm} C_{mm}^T$ as $d_{m\alpha} (\geq 0)$ ($\alpha = 1, \dots, N_m$). Then we obtain

$$\delta\lambda_{m\gamma}^1 = \begin{cases} 0 \\ \pm \frac{B_d}{r^{d-1}} \sqrt{d_{m\alpha}} \quad (\alpha = 1, \dots, N_m) \end{cases}. \quad (59)$$

Then $\sum_{m,\gamma} \delta\lambda_{m\gamma}^1 \frac{df}{d\lambda_m} \Big|_{\lambda_m = \lambda_m^0} = 0$, because we have $\sum_{\gamma} \delta\lambda_{m\gamma}^1 = 0$ from (58) and (59).

Next we consider $\delta\lambda_{m\gamma}^2$. We skip the detailed calculation because it is also almost similar to the time-independent perturbation theory with degeneracy of quantum mechanics. Then we can write $\delta\lambda_{m\gamma}^2$ as follows

$$\begin{aligned} \delta\lambda_{m\gamma}^2 &= \sum_{n(\neq m), i, \beta} \frac{1}{\lambda_m^0 - \lambda_n^0} (f_{ni\beta}^{0T} A^0 \delta\Lambda_1 \xi_{m\gamma}^0) (\xi_{m\gamma}^{0T} A^0 \delta\Lambda_1 f_{ni\beta}^0) \\ &= \sum_{n(\neq m)} \frac{1}{\lambda_m^0 - \lambda_n^0} \xi_{m\gamma}^{0T} A^0 \delta\Lambda_1 \hat{\phi}_n \delta\Lambda_1 \xi_{m\gamma}^0 \end{aligned} \quad (60)$$

where

$$\hat{\phi}_n \equiv \sum_{i, \beta} f_{ni\beta}^0 f_{ni\beta}^{0T} A^0. \quad (61)$$

$\hat{\phi}_n$ is a projection operator on the eigenspace of λ_n^0 . To obtain $\delta\lambda_{m\gamma}^2$ we must obtain $\xi_{m\gamma}^0$ by solving the eigenvalue problem, but it is not necessary for our purpose because we want to

know only $\sum_{m,\gamma} \delta\lambda_{m\gamma}^2 \frac{df}{d\lambda_m} \Big|_{\lambda_m=\lambda_m^0}$. From (60) we obtain

$$\begin{aligned}
\sum_{m,\gamma} \delta\lambda_{m\gamma}^2 \frac{df}{d\lambda_m} \Big|_{\lambda_m=\lambda_m^0} &= \sum_{m,\gamma} \sum_{n(\neq m)} \frac{1}{\lambda_m^0 - \lambda_n^0} \xi_{m\gamma}^{0T} A^0 \delta\Lambda_1 \hat{\phi}_n \delta\Lambda_1 \xi_{m\gamma}^0 \frac{df}{d\lambda_m} \Big|_{\lambda_m=\lambda_m^0} \\
&= \sum_{m,n(m\neq n)} \frac{1}{\lambda_m^0 - \lambda_n^0} \text{Tr}(\hat{\phi}_m \delta\Lambda_1 \hat{\phi}_n \delta\Lambda_1) \frac{df}{d\lambda_m} \Big|_{\lambda_m=\lambda_m^0} \\
&= \sum_{m,n(m>n)} \frac{1}{\lambda_m^0 - \lambda_n^0} \text{Tr}(\hat{\phi}_m \delta\Lambda_1 \hat{\phi}_n \delta\Lambda_1) \left(\frac{df}{d\lambda_m} \Big|_{\lambda_m=\lambda_m^0} - \frac{df}{d\lambda_n} \Big|_{\lambda_n=\lambda_n^0} \right).
\end{aligned} \tag{62}$$

In the second line we have used

$$\sum_{\gamma} \xi_{m\gamma}^0 \xi_{m\gamma}^{0T} A^0 = \hat{\phi}_m, \tag{63}$$

and in the third line we have used cyclic property of trace. Next we examine the sign of (62). Its trace term is positive because

$$\begin{aligned}
\text{Tr}(\hat{\phi}_m \delta\Lambda_1 \hat{\phi}_n \delta\Lambda_1) &= \sum_{i,\alpha,j,\beta} (f_{ni\alpha}^{0T} A^0 \delta\Lambda_1 f_{mj\beta}^0) (f_{mj\beta}^{0T} A^0 \delta\Lambda_1 f_{ni\alpha}^0) \\
&= \sum_{i,\alpha,j,\beta} V_{n\alpha m\beta}^{ij} V_{m\beta n\alpha}^{ji} = \sum_{i,\alpha,j,\beta} (V_{n\alpha m\beta}^{ij})^2 = 2 \left(\frac{B_d}{r^{d-1}} \right)^2 \sum_{\alpha,\beta} (C_{m\alpha n\beta})^2 \geq 0.
\end{aligned} \tag{64}$$

And from (19) we obtain

$$\frac{df}{d\lambda} = \frac{1}{2\sqrt{1+\lambda}} \ln \left[\sqrt{1+\frac{1}{\lambda}} + \frac{1}{\sqrt{\lambda}} \right] > 0 \quad \text{for } \lambda > 0, \tag{65}$$

$$\frac{d^2 f}{d\lambda^2} = -\frac{1}{4\sqrt{1+\lambda}} \left[\frac{1}{1+\lambda} \ln \left[\sqrt{1+\frac{1}{\lambda}} + \frac{1}{\sqrt{\lambda}} \right] + \frac{1}{\lambda\sqrt{1+\lambda}} \right] < 0 \quad \text{for } \lambda > 0. \tag{66}$$

From (64), (66) and $\lambda_m^0 > \lambda_n^0$ ($m > n$), (62) is negative. And from (66) we obtain

$$\sum_{m,\gamma} (\delta\lambda_{m\gamma}^1)^2 \frac{d^2 f}{d\lambda_m^2} \Big|_{\lambda_m=\lambda_m^0} \leq 0. \tag{67}$$

Finally, from (46), (58), (59), (62) and (64) we obtain

$$\begin{aligned}
S_{AB}(r, R_1, R_2) - S_A(R_1) - S_B(R_2) &= \sum_{m,\gamma} \left[\delta\lambda_{m\gamma}^2 \frac{df}{d\lambda_m} \Big|_{\lambda_m=\lambda_m^0} + \frac{1}{2} (\delta\lambda_m^1)^2 \frac{d^2f}{d\lambda_m^2} \Big|_{\lambda_m=\lambda_m^0} \right] \\
&= \left(\frac{B_d}{r^{d-1}} \right)^2 \left[\sum_{m,n(m>n)} \frac{2}{\lambda_m^0 - \lambda_n^0} \sum_{\alpha,\beta} (C_{m\alpha n\beta})^2 \left(\frac{df}{d\lambda_m} \Big|_{\lambda_m=\lambda_m^0} - \frac{df}{d\lambda_n} \Big|_{\lambda_n=\lambda_n^0} \right) \right. \\
&\quad \left. + \sum_{m',\alpha} c_{m'\alpha} \frac{d^2f}{d\lambda_m^2} \Big|_{\lambda_m=\lambda_{m'}^0} + \sum_{m'',\alpha} d_{m''\alpha} \frac{d^2f}{d\lambda_m^2} \Big|_{\lambda_m=\lambda_{m''}^0} \right] \equiv \frac{-1}{r^{2d-2}} G(R_1, R_2) \leq 0
\end{aligned} \tag{68}$$

where $\sum_{m'}$ denotes the summation taken over the common eigenvalues of Λ^{01} and Λ^{02} , whose degeneracy is $M_m \geq N_m$, and $\sum_{m''}$ denotes the summation taken over the common eigenvalues of Λ^{01} and Λ^{02} , whose degeneracy is $M_m < N_m$.

We have obtained the r dependence of $S_C(r, R_1, R_2) = S_{AB}(r, R_1, R_2)$ in (68), then we next consider $G(R_1, R_2)$. To calculate $G(R_1, R_2)$ we need to know λ_m^0 and $f_{mi\alpha}^0$ which we do not examine in this paper. But from $C_{m\alpha n\beta}(R_1 = 0, R_2) = C_{m\alpha n\beta}(R_1, R_2 = 0) = 0$ we obtain a trivial property of $G(R_1, R_2)$,

$$G(R_1 = 0, R_2) = G(R_1, R_2 = 0) = 0. \tag{69}$$

And $G(R_1, R_2)$ depends on the cutoff length l because λ_m^0 , $f_{mi\alpha}^0$ and $C_{m\alpha n\beta}$ depend on l . (λ_m^0 are dimensionless, so they depend on R_1/l or R_2/l . And in (55) $\int_A d^d z_a W(x_a, z_a)$ and $\int_B d^d z_b W(y_b, z_b)$ depend on l because $W(x, y)$ depend on l for $x \approx y$, so $C_{m\alpha n\beta}$ depends on l .) Probably $G(R_1, R_2)$ diverges when $l \rightarrow 0$, as $S_A(R_1)$ and $S_B(R_2)$ have $1/l^{d-1}$ divergence [1, 2]. And $G(R_1, R_2)$ most likely diverges more weakly than $S_A(R_1)$ and $S_B(R_2)$. Then, by dimensional analysis, when $R_1 = R_2 \equiv R$ we can assume

$$G(R_1 = R, R_2 = R) = g R^{2d-2} \left(\frac{R}{l} \right)^m \left(\ln \left(\frac{R}{l} \right) \right)^n \quad d-1 \geq m \geq 0, n \geq 0, g > 0 \tag{70}$$

where g is a dimensionless constant.

Finally we consider the condition under which the approximations are good. When $r \gg R_1, R_2$, $\delta\Lambda \approx \delta\Lambda_1$ is a good approximation. When $|\frac{B_d}{r^{d-1}} C_{m\alpha n\beta}| \ll |\lambda_m^0 - \lambda_n^0|$, the perturbation theory is a good approximation. The latter condition might have l dependence, so we might need the condition $R/r \ll (l/R)^a$, where $a \geq 0$.

$$\begin{aligned}
\tilde{\Lambda}_D &= - \left(\begin{array}{cc} \boxed{\text{diag}_1} + \boxed{\text{diag}_2} & \mathbf{0} \\ \mathbf{0} & \boxed{\text{diag}_3} + \boxed{\text{diag}_4} \end{array} \right) \\
\tilde{A} &= \left(\begin{array}{cc} \boxed{\text{diag}_5} & \mathbf{0} \\ \mathbf{0} & \boxed{\text{diag}_6} \end{array} \right) \\
\delta\tilde{\Lambda}_D &= \left(\begin{array}{cc} \boxed{\text{diag}_7} & \mathbf{0} \\ \mathbf{0} & \boxed{\text{diag}_8} \end{array} \right)
\end{aligned}$$

FIG. 8. The diagrammatic representations of $\tilde{\Lambda}_D$, \tilde{A} and $\delta\tilde{\Lambda}_D$.

VI. ENTANGLEMENT ENTROPY OF TWO BLACK HOLES IN A $d+1$ DIMENSIONAL MASSLESS FREE SCALAR FIELD

In this section we consider the entanglement entropy of the massless free scalar field on the outside region C of two black holes A and B whose radii are R_1 and R_2 . The action of the massless free scalar field is given by

$$S = -\frac{1}{2} \int d^d x \sqrt{-g} g^{\mu\nu} \nabla_\mu \phi \nabla_\nu \phi. \quad (71)$$

First we specify the vacuum state of the scalar field. The vacuum state is specified by specifying the time coordinate t . We use the coordinate system which have following properties: this coordinate system covers the inside and the outside regions of two black holes and does not have the coordinate singularity on the horizons and becomes the orthogonal coordinate system of Minkowski spacetime in the region far from the two black holes. To construct this coordinate system, we use the coordinates which is similar to the Kruskal coordinates in the inside regions and the neighborhood of black holes, and similar to the Schwarzschild coordinates in the other region. In this coordinate system g^{tt} is positive everywhere, then from (71) G_{MN} and V_{MN} in (10) are positive definite. So we can use the formalism in the Section IV.

We can use the method of the last section with some modifications. In the black hole case $W(x, y)$ and $W^{-1}(x, y)$ depend on r , so we write them as $W(x, y; r)$ and $W^{-1}(x, y; r)$. Exactly in the same way as in Minkowski spacetime, Eqs. (33)-(36) hold because (31) holds.

On the other hand $\Lambda_0 (= \lim_{r \rightarrow \infty} \Lambda)$ changes because $W(x, y; r)$ and $W^{-1}(x, y; r)$ depend on r . We define $W_A(x, y)$ and $W_A^{-1}(x, y)$ ($W_B(x, y)$ and $W_B^{-1}(x, y)$) as $W(x, y)$ and $W^{-1}(x, y)$ in the case that the only one black hole $A(B)$ exists. Then we have

$$\Lambda^0 = - \begin{pmatrix} \int_{A^c} d^d z W_A^{-1}(x_a, z) W_A(z, y_a) & 0 \\ 0 & \int_{B^c} d^d z W_B^{-1}(x_b, z) W_B(z, y_b) \end{pmatrix}. \quad (72)$$

It is difficult to evaluate the r dependence of $\delta\Lambda_D = \Lambda_D - \Lambda^0$ because it is difficult to evaluate $W(x, y; r) - W_{A(B)}(x, y)$ and $W^{-1}(x, y; r) - W_{A(B)}^{-1}(x, y)$. So, in the black hole case we *do not* consider Λ_0 as the non-perturbative part. Instead we define $\tilde{\Lambda}_D(r)$ and $\tilde{A}(r)$ as (see Fig 8)

$$\begin{aligned} \tilde{\Lambda}_D(r) &\equiv \begin{pmatrix} \Lambda_A(x_a, y_a; r) & 0 \\ 0 & \Lambda_B(x_b, y_b; r) \end{pmatrix} \\ &\equiv \begin{pmatrix} - \int_{A^c} d^d z W^{-1}(x_a, z; r) W(z, y_a; r) & 0 \\ 0 & - \int_{B^c} d^d z W^{-1}(x_b, z; r) W(z, y_b; r) \end{pmatrix}, \end{aligned} \quad (73)$$

$$\tilde{A}(r) \equiv \begin{pmatrix} W(x_a, y_a; r) & 0 \\ 0 & W(x_b, y_b; r) \end{pmatrix}, \quad (74)$$

and we consider $\tilde{\Lambda}_D$ as the non-perturbative part. Note that Λ_A and Λ_B are the matrices Λ corresponding to $S_A(r, R_1, R_2)$ and $S_B(r, R_1, R_2)$. So we will obtain S_{AB} as the following form, $S_{AB}(r, R_1, R_2) = S_A(r, R_1, R_2) + S_B(r, R_1, R_2) + \delta S_{AB}(r, R_1, R_2)$. We calculate the leading term of $\delta S_{AB}(r, R_1, R_2)$ with respect to $1/r$.

We define $\delta\tilde{\Lambda}_D \equiv \Lambda_D - \tilde{\Lambda}_D$ (see Fig 8), then we have $\Lambda = \tilde{\Lambda}_D + \delta\Lambda_1 + \delta\Lambda_2 + \delta\tilde{\Lambda}_D$. To evaluate $\delta\Lambda_1$, $\delta\Lambda_2$ and $\delta\tilde{\Lambda}_D$, we evaluate $W(x_a, y_b; r)$ and $W^{-1}(x_a, y_b; r)$. When $r \gg R_1, R_2$, by dimensional analysis we obtain $W(x_a, y_b; r) \approx \frac{A_d}{r^{d+1}} L_1(R_1/r, R_2/r)$ and $W^{-1}(x_a, y_b; r) \approx \frac{B_d}{r^{d-1}} L_2(R_1/r, R_2/r)$, where L_1 and L_2 are dimensionless functions of R_1/r and R_2/r . The space time becomes Minkowski space time when $R_1 \rightarrow 0$ and $R_2 \rightarrow 0$, so in this limit probably we have $L_1 \rightarrow 1$ and $L_2 \rightarrow 1$. This limit is equivalent to $r \rightarrow \infty$, so we have $\lim_{r \rightarrow \infty} L_1 = \lim_{r \rightarrow \infty} L_2 = 1$. Then we obtain $\delta\Lambda_1 = O(1/r^{d-1})$, $\delta\Lambda_2 = O(1/r^{d+1})$ and $\delta\tilde{\Lambda}_D = O(1/r^{2d})$ as well as the Minkowski spacetime case. We can neglect $\delta\Lambda_2$ and $\delta\tilde{\Lambda}_D$ for the same reason as in the Minkowski spacetime case (see below Eq.(42)). So we can approximate $\Lambda \approx \tilde{\Lambda}_D + \delta\Lambda_1$. Then we change the perturbative calculation in the last section as follow

$$\Lambda^0 \rightarrow \tilde{\Lambda}_D(r) \quad A^0 \rightarrow \tilde{A}(r) \quad \lambda_m^0 \rightarrow \tilde{\lambda}_m^0(r) \quad f_{mi\alpha}^0 \rightarrow \tilde{f}_{mi\alpha}^0(r) \quad (75)$$

where $\tilde{\lambda}_m^0(r)$ and $\tilde{f}_{mi\alpha}^0(r)$ are the eigenvalues and the eigenvectors of $\tilde{\Lambda}_D(r)$. The perturbative calculation is the same as that in the last section. In this case $\tilde{A}(r)$, $\tilde{\lambda}_m^0(r)$ and $\tilde{f}_{mi\alpha}^0(r)$ depend on r , but we can remove their r dependence as follow. Because we want to calculate the leading term of $S_{AB}(r, R_1, R_2) - S_A(r, R_1, R_2) - S_B(r, R_1, R_2)$ with respect to $1/r$, we can approximate

$$\begin{aligned} \tilde{A}\delta\Lambda_1 &\approx \frac{B_d L_2\left(\frac{R_1}{r}, \frac{R_2}{r}\right)}{r^{d-1}} \begin{pmatrix} 0 & \int_A d^d z_a W(x_a, z_a; r) \int_B d^d z_b W(z_b, y_b; r) \\ \int_B d^d z_b W(x_b, z_b; r) \int_A d^d z_a W(z_a, y_a; r) & 0 \end{pmatrix} \\ &\approx \frac{B_d}{r^{d-1}} \begin{pmatrix} 0 & \int_A d^d z_a W_A(x_a, z_a) \int_B d^d z_b W_B(z_b, y_b) \\ \int_B d^d z_b W_B(x_b, z_b) \int_A d^d z_a W_A(z_a, y_a) & 0 \end{pmatrix} \end{aligned} \quad (76)$$

In the second line we have approximated $L_2\left(\frac{R_1}{r}, \frac{R_2}{r}\right) \approx 1$, $W(x_a, z_a; r) \approx W_A(x_a, z_a)$ and $W(z_b, y_b; r) \approx W_B(z_b, y_b)$. And we can approximate $\tilde{\lambda}_m^0(r) \approx \tilde{\lambda}_m^0(r = \infty) \equiv \lambda_m^0$ and $\tilde{f}_{mi\alpha}^0(r) \approx \tilde{f}_{mi\alpha}^0(r = \infty) \equiv f_{mi\alpha}^0$. Note that λ_m^0 and $f_{mi\alpha}^0$ are the eigenvalues and the eigenvectors of Λ^0 , i.e. (Λ^0 is in (72))

$$f_{m1\alpha}^0 = \begin{pmatrix} f_{m1\alpha}^0(x_a) \\ 0 \end{pmatrix}, f_{n2\beta}^0 = \begin{pmatrix} 0 \\ f_{n2\beta}^0(x_b) \end{pmatrix}, \Lambda^0 f_{m1\alpha}^0 = \lambda_m^0 f_{m1\alpha}^0, \Lambda^0 f_{n2\beta}^0 = \lambda_n^0 f_{n2\beta}^0, \quad (77)$$

where $\alpha = 1, \dots, M_m$ and $\beta = 1, \dots, N_n$ are the labels of the degeneracy.

Finally we obtain

$$S_{AB}(r, R_1, R_2) = S_A(r, R_1, R_2) + S_B(r, R_1, R_2) - \frac{1}{r^{2d-2}} G(R_1, R_2) \quad (78)$$

where $G(R_1, R_2)$ is the same function as that in (68). Note that in this case from (76) $C_{m\alpha n\beta}$ in $G(R_1, R_2)$ is

$$C_{m\alpha n\beta} = \int_A d^d x_a \int_A d^d z_a W_A(x_a, z_a) f_{m1\alpha}^0(x_a) \int_B d^d y_b \int_B d^d z_b W_B(y_b, z_b) f_{n2\beta}^0(y_b). \quad (79)$$

As in the Minkowski spacetime case, we obtain $G(R_1 = 0, R_2) = G(R_1, R_2 = 0) = 0$ from $C_{m\alpha n\beta}(R_1 = 0, R_2) = C_{m\alpha n\beta}(R_1, R_2 = 0) = 0$, and $G(R_1, R_2)$ probably diverges when $l \rightarrow 0$, where l is the cutoff length. The $1/l$ dependence of $G(R_1, R_2)$ is most likely the same as that in the Minkowski spacetime, then we obtain

$$G(R_1 = R, R_2 = R) = g_{BH} R^{2d-2} \left(\frac{R}{l}\right)^m \left(\ln\left(\frac{R}{l}\right)\right)^n \quad d-1 \geq m \geq 0, n \geq 0, g_{BH} > 0 \quad (80)$$

where g_{BH} is a dimensionless constant, and m and n are the same numbers as those in the Minkowski spacetime.

VII. ENTANGLEMENT ENTROPIC FORCE AND THE PHYSICAL PREDICTION

We *assume* that we can consider the entanglement entropy of two black holes as thermodynamic entropy. If this assumption is correct, the entropic force acts on two black holes. We consider the force of the scalar field which acts on two black holes. We consider two black holes which have same radius $R_1 = R_2 \equiv R$, then we can consider the temperature T to be the Hawking temperature. We define the energy and the free energy of the field on the region C as $E_C(r, R)$ and $F_C(r, R)$,

$$F_C(r, R) = E_C(r, R) - TS_C(r, R) = E_C(r, R) - T \left(2S_A(r, R) - \frac{1}{r^{2d-2}}G(R) \right). \quad (81)$$

where $G(R) \equiv G(R_1 = R, R_2 = R)$ and we have used (78). We define the force of the field on the region C which acts on one black hole in the direction of increasing r as X_C . We obtain X_C by partially differentiating F_C with R fixed,

$$X_C(r, R) = -\frac{\partial F_C}{\partial r} = -\frac{\partial E_C(r, R)}{\partial r} + T \left(2\frac{\partial S_A(r, R)}{\partial r} + (2d-2)\frac{1}{r^{2d-1}}G(R) \right). \quad (82)$$

In (82) the second term is the entropic force.

We cannot see the effect of the entropic force only from (82) because we do not know $S_A(r, R)$. To see the effect of the entropic force we consider three situations. (See Fig 9) (1) There are two black holes which have the same radius R and the distance between them is r . (This is the situation we have considered.) (2) There are one black hole whose radius is R and one solid ball whose radius is $R_0 \approx R$ ($R_0 > R$), and the distance between them is r . This ball has mass M which is the same as that of a black hole whose radius is R . And the scalar field does not exist in this ball. The boundary condition on the scalar field on the surface of this ball is not so important in the later calculation that we do not specify the boundary condition in detail. We only require that the scalar field on the outside region of this ball is not so different from that in the situation (1). (3) There are two solid balls which have the same radius R_0 and the distance between them is r . These balls have the same properties as those in the situation (2).

We define the force of the field which acts on one black hole or on one ball in the direction of increasing r as $X_C^{(1)}$, $X_{C_2}^{(2)}$ and $X_{C_3}^{(3)}$. We illustrate in Fig 9 the directions of force and the names of the regions.

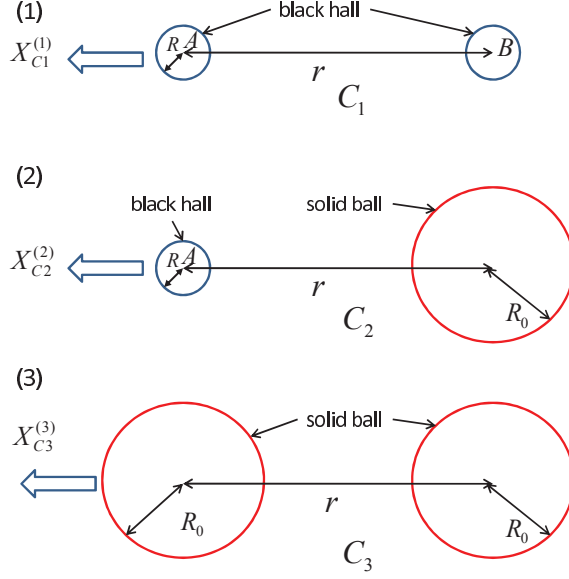


FIG. 9. Three situations to see the effect of the entropic force. (1) There are two black holes. (2) There are one black hole and one solid ball. (3) There are two solid balls. We define the force of the field which acts on one black hole or on one ball in the direction of increasing r as $X_C^{(1)}$, $X_{C_2}^{(2)}$ and $X_{C_3}^{(3)}$.

In the situation (2) the state of the field is $|0\rangle_{A+C_2}^{(2)}$, where $|0\rangle_{A+C_2}^{(2)}$ is the vacuum state on $A + C_2$. Because $|0\rangle_{A+C_2}^{(2)}$ is a pure state, then $S_{C_2}^{(2)} = S_A^{(2)}$. We define $\Lambda_A^{(1)}$ ($\Lambda_A^{(2)}$) as Λ corresponding to $S_A^{(1)}$ ($S_A^{(2)}$). Because the scalar field does not exist in the ball, then we obtain

$$\Lambda_A^{(2)} - \Lambda_A^{(1)} \approx \int_B d^d z_b W^{-1}(x_a, z_b) W(z_b, y_a) = O\left(\frac{1}{r^{2d}}\right). \quad (83)$$

Then we can approximate $S_A^{(2)} = S_A^{(1)}(r, R) + O(\frac{1}{r^{2d}}) \approx S_A^{(1)}(r, R)$. Then we obtain

$$X_{C_2}^{(2)}(r, R) = -\frac{\partial F_{C_2}^{(2)}}{\partial r} = -\frac{\partial E_{C_2}^{(2)}(r, R)}{\partial r} + T \frac{\partial S_A^{(2)}(r, R)}{\partial r} \approx -\frac{\partial E_{C_2}^{(2)}(r, R)}{\partial r} + T \frac{\partial S_A^{(1)}(r, R)}{\partial r}. \quad (84)$$

In the situation (3) the state of the field on the region C_3 is a pure state, so $S_{C_3}^{(3)} = 0$. Then we obtain

$$X_{C_3}^{(3)}(r, R) = -\frac{\partial F_{C_3}^{(3)}}{\partial r} = -\frac{\partial E_{C_3}^{(3)}(r, R)}{\partial r}. \quad (85)$$

From (82) (84) and (85) we obtain

$$X_{C_1}^{(1)} - 2X_{C_2}^{(2)} + X_{C_3}^{(3)} \approx -\frac{\partial}{\partial r} [E_{C_1}^{(1)} - 2E_{C_2}^{(2)} + E_{C_3}^{(3)}] + (2d - 2)T \frac{1}{r^{2d-1}} G(R). \quad (86)$$

$E_{C_1}^{(1)} - 2E_{C_2}^{(2)} + E_{C_3}^{(3)}$ is Casimir energy.

We have not considered the force of gravity. But we can include them in (86) easily. We define total force acting on one black hole or on one ball in the direction of increasing r as $\mathcal{F}_A^{(1)}$, $\mathcal{F}_A^{(2)}$ and $\mathcal{F}_{ball}^{(3)}$. Then we obtain

$$\mathcal{F}_A^{(1)} - 2\mathcal{F}_A^{(2)} + \mathcal{F}_{ball}^{(3)} = X_{C_1}^{(1)} - 2X_{C_2}^{(2)} - X_{C_3}^{(3)} \approx -\frac{\partial}{\partial r}[E_{C_1}^{(1)} - 2E_{C_2}^{(2)} + E_{C_3}^{(3)}] + (2d-2)T\frac{1}{r^{2d-1}}G(R). \quad (87)$$

The force of gravity is canceled in (87). The first and the second terms in the right hand side are the Casimir force and the effect of entropic force, respectively.

Finally we consider the case $d = 3$. In this case the Hawking temperature is $T = \frac{1}{8\pi G_N M} = \frac{1}{4\pi R}$. From (80) and (87) we obtain

$$\mathcal{F}_A^{(1)} - 2\mathcal{F}_A^{(2)} + \mathcal{F}_{ball}^{(3)} \approx -\frac{\partial}{\partial r}[E_{C_1}^{(1)} - 2E_{C_2}^{(2)} + E_{C_3}^{(3)}] + \frac{g_{BH}}{\pi} \frac{R^3}{r^5} \left(\frac{R}{l}\right)^m \left(\ln\left(\frac{R}{l}\right)\right)^n \quad (88)$$

$$2 \geq m \geq 0, n \geq 0, g_{BH} > 0.$$

We roughly estimate the Casimir force by analogy with that of electromagnetic field between two dielectric spheres with center-to-center distance r in Minkowski spacetime. The Casimir force between the two sphere was calculated in [22], and it is $O(1/r^8)$. So, in our case we can probably neglect $-\frac{\partial}{\partial r}[E_{C_1}^{(1)} - 2E_{C_2}^{(2)} + E_{C_3}^{(3)}]$ in (88). The left hand side of (88) can be measured experimentally, so (88) is the physical prediction. From (88) the effect of the entropic force becomes significant when R is large. We can probably use heavy stars as the balls in the situation (2) and (3). So we can possibly confirm the effect of the entropic force by the cosmic observation (e.g. binary black holes and binary neutron stars).

We estimate the magnitude of the effect of the entropic force. We set the cutoff length l to the Planck length $l_P = (G_N \hbar / c^3)^{1/2}$, then the ratio of the effect of the entropic force to the force of gravity is

$$\frac{\mathcal{F}_{eff}}{\mathcal{F}_g} = \frac{-4g_{BH}}{\pi} \frac{(l_P)^2 R}{r^3} \left(\frac{R}{l_P}\right)^m \left(\ln\left(\frac{R}{l_P}\right)\right)^n \quad (89)$$

where

$$\mathcal{F}_{eff} \equiv \frac{\hbar c g_{BH}}{\pi} \frac{R^3}{r^5} \left(\frac{R}{l_P}\right)^m \left(\ln\left(\frac{R}{l_P}\right)\right)^n \quad \mathcal{F}_g \equiv -\frac{G_N M^2}{r^2} = -\frac{c^4 R^2}{4G_N r^2}. \quad (90)$$

VIII. NUMERICAL STUDIES OF ENTANGLEMENT ENTROPY IN A MASSLESS FREE SCALAR FIELD IN $(d + 1)$ -DIMENSIONAL MINKOWSKI SPACE-TIME: LATTICE FORMULATION

We could not obtain the explicit form of $G(R_1, R_2)$ in (68) analytically. Next we calculate $G(R_1, R_2)$ numerically. We apply the formalism of Bombelli et al [1] reviewed in Section IV to a massless free scalar field in $(d + 1)$ -dimensional Minkowski spacetime. The Lagrangian is given by

$$L = \int d^d x \frac{1}{2} [\dot{\phi}^2 - (\nabla\phi)^2]. \quad (91)$$

As an ultraviolet regulator, we replace the continuous d -dimensional space coordinates x by a lattice of discrete points with spacing a . As an infrared cutoff, we allow the individual components of $n \equiv x/a$ to assume only a finite number N of independent values $-N/2 < n_\mu \leq N/2$. The Greek indices denoting vector quantities run from one to d . Outside this range we assume the lattice is periodic. The dimensionless Hamiltonian $H_0 \equiv aH$ is given by

$$H_0 \equiv aH = \sum_n \left[\frac{1}{2} \pi_n^2 + \frac{1}{2} \sum_{\mu=1}^d (\phi_{n_\nu + \delta_{\nu\mu}} - \phi_{n_\nu})^2 + \frac{a^2 m^2}{2} \phi_n^2 \right] \equiv \sum_n \frac{1}{2} \pi_n^2 + \sum_{m,n} \frac{1}{2} \phi_m V_{mn} \phi_n, \quad (92)$$

where ϕ_n and π_n are dimensionless and Hermitian, and obey the canonical commutation relations

$$[\phi_n, \pi_m] = i\delta_{nm}. \quad (93)$$

In Eq.(92) we insert a mass term in order to remove a zero eigenvalue of V_{mn} ; if V_{mn} should have the zero eigenvalue, W^{-1} in (15) would not exist. Later we will take N to infinity. In this limit we can neglect the zero eigenvalue of V_{mn} and will take am to zero. Taking N to infinity is important in order to calculate the entanglement entropy S_{AB} of two spheres. The entanglement entropy of two spheres is more sensitive to the value of N than that of one sphere. (In fact, we numerically calculated S_{AB} for finite N with antiperiodic boundary conditions without the mass term. S_{AB} depends on N when the distance r between two spheres is close to $N/2$, and we could not obtain the clear r dependence of S_{AB} .)

From (92) we obtain (see e.g. [21])

$$W_{mn} = N^{-d} \sum_k [a^2 m^2 + 2 \sum_{\mu=1}^d (1 - \cos \frac{2\pi k_\mu}{N})]^{1/2} e^{2\pi i k(n-m)/N}, \quad (94)$$

$$W_{mn}^{-1} = N^{-d} \sum_k [a^2 m^2 + 2 \sum_{\mu=1}^d (1 - \cos \frac{2\pi k_\mu}{N})]^{-1/2} e^{2\pi i k(n-m)/N}, \quad (95)$$

where the index k also carries d integer valued components, each in the range of $-N/2 < k_\mu \leq N/2$. We take N to infinity and change the momentum sum into an integral with the replacements $q_\mu = 2\pi k_\mu/N$ and $N^{-d} \sum_k \rightarrow \int_{-\pi}^{\pi} \frac{d^d q}{(2\pi)^d}$, and then we have

$$W_{mn} = \int_{-\pi}^{\pi} \frac{d^d q}{(2\pi)^d} e^{iq(n-m)} [a^2 m^2 + 2 \sum_{\mu=1}^d (1 - \cos q_\mu)]^{\frac{1}{2}}, \quad (96)$$

$$W_{mn}^{-1} = \int_{-\pi}^{\pi} \frac{d^d q}{(2\pi)^d} e^{iq(n-m)} [a^2 m^2 + 2 \sum_{\mu=1}^d (1 - \cos q_\mu)]^{\frac{-1}{2}}. \quad (97)$$

In (96) and (97) the integrals converge when $am \rightarrow 0$, so we can take am to zero,

$$W_{mn} = \int_{-\pi}^{\pi} \frac{d^d q}{(2\pi)^d} e^{iq(n-m)} [2 \sum_{\mu=1}^d (1 - \cos q_\mu)]^{\frac{1}{2}}, \quad (98)$$

$$W_{mn}^{-1} = \int_{-\pi}^{\pi} \frac{d^d q}{(2\pi)^d} e^{iq(n-m)} [2 \sum_{\mu=1}^d (1 - \cos q_\mu)]^{\frac{-1}{2}}. \quad (99)$$

From (98) and (99) we can compute W_{mn} and W_{mn}^{-1} numerically. Then we can compute the entanglement entropy from (18), (19) and (20). The integrands in (98) and (99) highly oscillate when $\|n - m\| \gg 1$, and the numerical integrals converge very slowly. We can obtain approximate expressions of W_{mn} and W_{mn}^{-1} by hand when $\|n - m\| \gg 1$, so we will use them when $\|n - m\| \gg 1$ in order to reduce the computational complexity of W_{mn} and W_{mn}^{-1} . To evaluate W_{mn} and W_{mn}^{-1} when $\|n - m\| \gg 1$, we define $r \equiv a(n - m)$ and take $\|n - m\|$ to infinity keeping r fixed. We change the variable as $p = q/a$, and then we have

$$W_{mn} = a^d \int_{-\frac{\pi}{a}}^{\frac{\pi}{a}} \frac{d^d p}{(2\pi)^d} e^{ipr} [2 \sum_{\mu=1}^d (1 - \cos ap_\mu)]^{\frac{1}{2}} \rightarrow a^{d+1} \int_{-\infty}^{\infty} \frac{d^d p}{(2\pi)^d} e^{ipr - \frac{a}{\pi} \|p\|} [\|p\|^2]^{\frac{1}{2}}. \quad (100)$$

We can perform the integral in (100) analytically when $\|r\|/a \rightarrow \infty$ (see Appendix A), and then we obtain

$$W_{mn} \rightarrow a^{d+1} \frac{A_d}{\|r\|^{d+1}} = \frac{A_d}{\|n - m\|^{d+1}}, \quad (101)$$

where

$$A_d = \begin{cases} -\frac{(d-1)!!}{(2\pi)^{d/2}} & \text{for even } d \geq 2, \\ -2\frac{(d-1)!!}{(2\pi)^{(d+1)/2}} & \text{for odd } d \geq 3. \end{cases} \quad (102)$$

We can evaluate W_{mn}^{-1} when $\|n - m\| \gg 1$ in the same way (see Appendix A), and then we obtain

$$W_{mn}^{-1} \rightarrow a^{d-1} \int_{-\infty}^{\infty} \frac{d^d p}{(2\pi)^d} e^{i p r - \frac{a}{\pi} \|\vec{p}\| [\|\vec{p}\|^2]^{\frac{-1}{2}}} \rightarrow a^{d-1} \frac{B_d}{\|r\|^{d-1}} = \frac{B_d}{\|n - m\|^{d-1}}. \quad (103)$$

where

$$B_d = \begin{cases} \frac{(d-3)!!}{(2\pi)^{d/2}} & \text{for even } d \geq 2, \\ 2 \frac{(d-3)!!}{(2\pi)^{(d+1)/2}} & \text{for odd } d \geq 3, \end{cases} \quad (104)$$

where $0!! = (-1)!! = 1$.

IX. NUMERICAL CALCULATIONS

We calculate numerically the entanglement entropy S_{AB} of two spheres A and B whose radii are R_1 and R_2 , and the distance between the centers of them is r for $d = 3$.

We put the centers of the spheres on a lattice. We define the sphere whose radius is R as a set of points which are at distances of R or less from the center of the sphere. In order to reduce the computational complexity of W_{mn} and W_{mn}^{-1} , we use the approximate expressions (101) and (103) when $\|n - m\| > 10$, and we use the numerical integrals of exact expressions (98) and (99) when $\|n - m\| \leq 10$. When $\|n - m\| = 10$, the differences between the numerical integrals of the exact expressions and the approximate expressions are less than 4% for W_{mn} and less than 1% for W_{mn}^{-1} . We perform matrix operations and calculate the eigenvalues λ_n of the matrix Λ in (20) with `Mathematica 8`. The number of columns and rows of Λ is the number of points in the region of which we calculate entanglement entropy.

We show the computed values of $S(R)$ which is the entanglement entropy of one sphere as a function of R^2/a^2 in Fig.10, where a is a lattice spacing. The points are fitted by a straight line:

$$S = 0.37R^2/a^2. \quad (105)$$

This result agrees with the result in [2] except for the coefficient. (The coefficient in [2] is 0.30. This difference necessarily arises from the difference of regularization methods. In [2] the author use the polar coordinate system and replace the continuous radial coordinate by a lattice.)

We show the computed values of $S_{AB}(r, R_1, R_2)$ which is the entanglement entropy of two spheres as a function of r/a for $R_1/a = R_2/a = 6, 7$ in Fig.11. As can be seen, S_{AB} reaches its maximum value $S_A + S_B$ when $r \rightarrow \infty$. In order to clarify the behavior of S_{AB} as a function of r , we show the computed values of $(S_A + S_B - S_{AB})^{-1/4}(r, R_1, R_2)$ as a function of r/a for $R_1/a = R_2/a = 6, 7$ in Fig.12. The straight lines in Fig.12 are fitted by the data between $r/a = R_1/a + R_2/a + 24$ and $r/a = R_1/a + R_2/a + 84$. In these regions the points are beautifully fitted by the straight lines. Then, when $r \gg R_1, R_2$, we obtain

$$-S_{A;B} \equiv S_{AB}(r, R_1, R_2) - S_A(R_1) - S_B(R_2) \approx -\frac{G(R_1, R_2)}{r^4}, \quad (106)$$

where $G(R_1, R_2)$ is defined in (106) and $G(R_1, R_2) = G(R_2, R_1) \geq 0$. $S_{A;B}$ is the mutual information of A and B . From Fig.12 the approximate expression (106) is precise for relatively small r . (When $R_1 = R_2 \equiv R$, for $r \gtrsim 3R$ (106) is precise from Fig.12.) We can obtain $G(R_1, R_2)/a^4$ from slopes of graphs of $(S_A + S_B - S_{AB})^{-1/4}(r, R_1, R_2)$, and then we show the computed values of $G(R_1, R_2)/a^4$ as a function of R_2^2/a^2 for $R_1/a = 4, 4.5, \dots, 7$ in Fig.13. From Fig.13 we can see that $G(R_1, R_2)/a^4$ is proportional to R_2^2 . Because $G(R_1, R_2) = G(R_2, R_1)$, we obtain $G(R_1, R_2) = gR_1^2R_2^2$, where g is a dimensionless constant. We can obtain the values of gR_1^2 from slopes of graphs of $G(R_1, R_2)$ as a function of R_2^2 . To obtain the precise value of g , we show the computed values of gR_1^2/a^2 as a function of R_1^2/a^2 in Fig.14 and obtain $g = 0.26$ from the slope of the line which is the best linear fit in Fig.14.

Finally, when $r \gg R_1, R_2$, we obtain

$$-S_{A;B} = S_{AB}(r, R_1, R_2) - S_A(R_1) - S_B(R_2) \approx -\frac{0.26R_1^2R_2^2}{r^4}. \quad (107)$$

When $r \approx R_1, R_2$, from Fig.12, S_{AB} rapidly decreases when r decreases. (Note that we cannot determine the functional form of $G(R_1, R_2)$ only by the constraints from dimensional analysis, symmetry, and behavior in the limit $R_1 \rightarrow 0$. For example, $G(R_1, R_2) = R_1^3R_2 + R_1R_2^3$ is not prohibited by these constraints.)

For $d = 2$, we compute S_{AB} in the same way. We show only the computed values of $(S_A + S_B - S_{AB})^{-1/2}(r, R_1, R_2)$ as a function of r/a for $R_1/a = R_2/a = 15, 16$ in Fig.15. The straight lines in Fig.15 are fitted by the data between $r/a = R_1/a + R_2/a + 101$ and $r/a = R_1/a + R_2/a + 201$. In these regions the points are beautifully fitted by the straight lines. We cross-checked our numerical procedure with the data of related calculations in

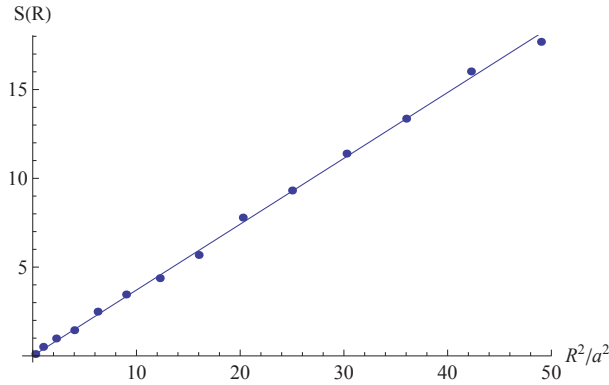


FIG. 10. The entanglement entropy $S(R)$ of one sphere whose radius is R as a function of R^2/a^2 . The line is the best linear fit.

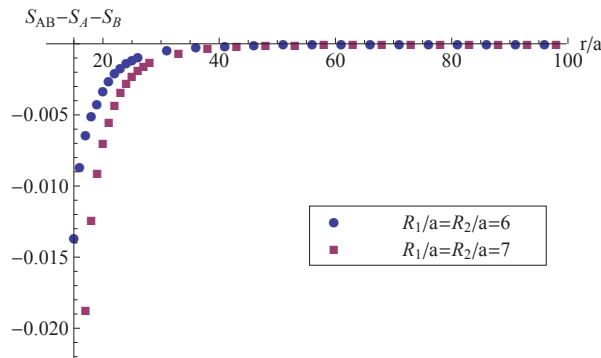


FIG. 11. $S_{AB} - S_A - S_B$ as a function of r/a for $R_1/a = R_2/a = 6, 7$, where S_{AB} is the entanglement entropy of two spheres A and B whose radii are R_1 and R_2 . The distance between the centers of the two spheres is r .

Figure 1 in [19]. (In the figure, the authors show the mutual information of two discs for $R_1 = R_2 = R$ and $r = 3R$. Our results were very close to theirs.) Finally, when $r \gg R_1, R_2$, we obtain

$$-S_{A;B} = S_{AB}(r, R_1, R_2) - S_A(R_1) - S_B(R_2) \approx -\frac{0.37R_1R_2}{r^2}. \quad (108)$$

In order to examine whether only the degrees of freedom on the surface of the spheres contribute to the mutual information or not, we calculate the mutual information $S_{D;E}$ of two same spherical shells D and E for $d = 3$ and the mutual information $S_{H;I}$ of two same rings H and I for $d = 2$. The internal (external) radii of the spherical shell and the ring are L_1 (L_2). The distance between the centers of the two spherical shells and that between the two rings are r . When $r \gg L_2$, we obtain $S_{D;E} \approx G_{ss}(L_1, L_2)/r^4$ and $S_{H;I} \approx G_r(L_1, L_2)/r^2$. We show

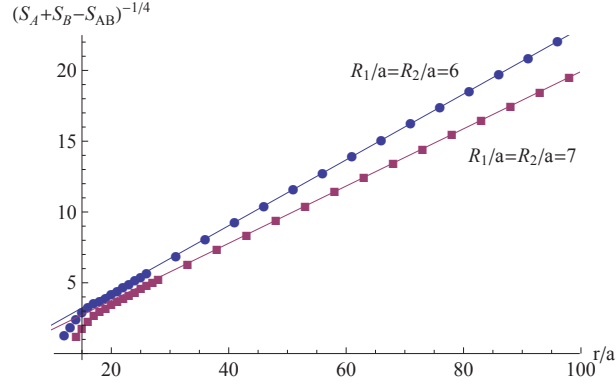


FIG. 12. $(S_A + S_B - S_{AB})^{-1/4}$ as a function of r/a for $R_1/a = R_2/a = 6, 7$, where S_{AB} is the entanglement entropy of two spheres A and B whose radii are R_1 and R_2 . The distance between the centers of the two spheres is r . The straight lines are fitted by the data between $r/a = R_1/a + R_2/a + 24$ and $r/a = R_1/a + R_2/a + 84$. For $r \gtrsim 3R (\equiv R_1 = R_2)$ the lines are beautifully fitted and the approximate expressions (106) and (107) are precise.

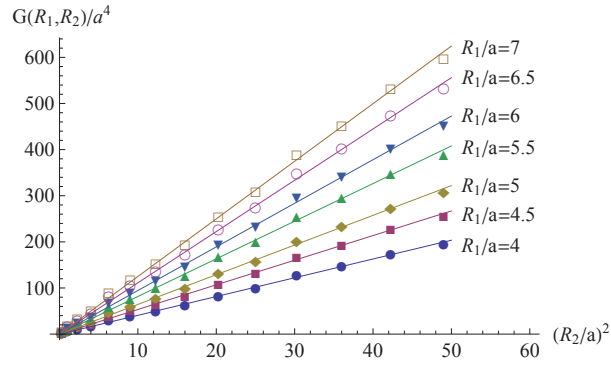


FIG. 13. $G(R_1, R_2)/a^4$ in (106) as a function of R_2^2/a^2 for $R_1/a = 4, 4.5, \dots, 7$. The lines are the best linear fit.

$(G_{ss}(L_1, L_2))^{1/2}/L_2^2$ for $L_2 = 10a$ as a function of L_1/L_2 in Fig.16 and $(G_r(L_1, L_2))^{1/2}/L_2$ for $L_2 = 22a$ as a function of L_1/L_2 in Fig.17. The curve in Fig.16 is $0.50(1 - (L_1/L_2)^3)^{2/3}$ and the curve in Fig.17 is $0.56(1 - (L_1/L_2)^2)^{1/2}$. We show these curves for comparison with the data. From Fig.16 and Fig.17, $(G_{ss}(L_1, L_2))^{1/2}/L_2^2$ and $(G_r(L_1, L_2))^{1/2}/L_2$ are monotone decreasing function of L_1/L_2 , and $(G_{ss}(L_1, L_2))^{1/2}$ is not proportional to the $2/3$ power of the volume of the spherical shell, and $(G_r(L_1, L_2))^{1/2}$ is not proportional to the $1/2$ power of the area of the ring. Then not only the degrees of freedom on the surface of the sphere but also those on the inside region contribute to the mutual information, and the degrees of

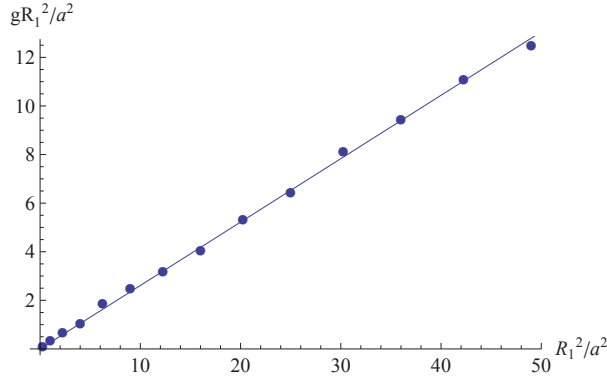


FIG. 14. gR_1^2/a^2 as a function of R_1^2/a^2 , where g is defined as $G(R_1, R_2) = gR_1^2R_2^2$. The line is the best linear fit.

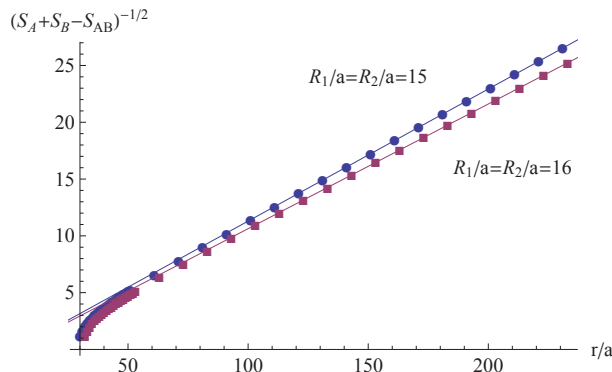


FIG. 15. $(S_A + S_B - S_{AB})^{-1/2}$ as a function of r/a for $R_1/a = R_2/a = 15, 16$, where S_{AB} is the entanglement entropy of two discs A and B whose radii are R_1 and R_2 . The distance between the centers of the two discs is r . The straight lines are fitted by the data between $r/a = R_1/a + R_2/a + 101$ and $r/a = R_1/a + R_2/a + 201$. For $r \gtrsim 4R (\equiv R_1 = R_2)$ the lines are beautifully fitted and the approximate expression (108) is precise.

freedom on the inside region does not contribute uniformly to the mutual information.

We roughly estimate the magnitude of the entropic force between two black holes by using S_{AB} in Minkowski spacetime. We consider two black holes (A and B) which have the same radius $R_1 = R_2 \equiv R$ and the distance between which is r . For simplicity, we consider the case that the state of the field on the whole space is a pure state. Generally, if a composite system XY is in a pure state, then $S_X = S_Y$ [14]. Then the entanglement entropy of the outside region of two black holes is equal to that of the inside regions of two black holes. We define the entropic force of the field on the outside region which acts on one black hole

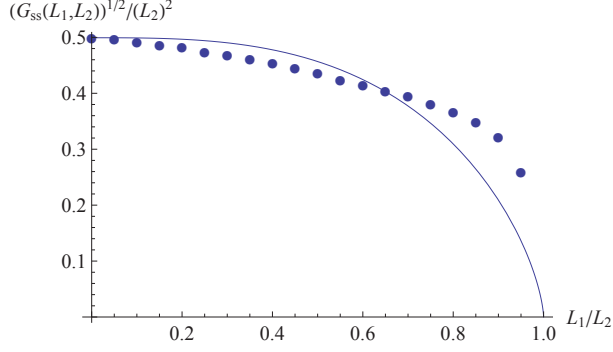


FIG. 16. $(G_{ss}(L_1, L_2))^{1/2}/L_2^2$ for $L_2 = 10a$ as a function of L_1/L_2 . $G_{ss}(L_1, L_2)$ is defined as $S_{D;E} \approx G_{ss}(L_1, L_2)/r^4$ when $r \gg L_1, L_2$. The curve is $0.50(1 - (L_1/L_2)^3)^{2/3}$. $(G_{ss}(L_1, L_2))^{1/2}/L_2^2$ is monotone decreasing function of L_1/L_2 and not proportional to $(1 - (L_1/L_2)^3)^{2/3}$.

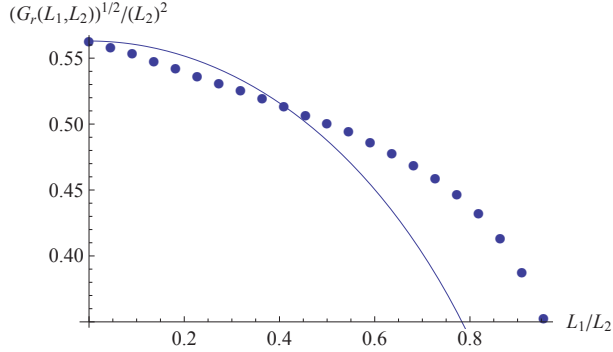


FIG. 17. $(G_r(L_1, L_2))^{1/2}/L_2^2$ for $L_2 = 22a$ as a function of L_1/L_2 . $G_r(L_1, L_2)$ is defined as $S_{H;I} \approx G_r(L_1, L_2)/r^2$ when $r \gg L_1, L_2$. The curve is $0.56(1 - (L_1/L_2)^2)^{1/2}$. $(G_r(L_1, L_2))^{1/2}/L_2^2$ is monotone decreasing function of L_1/L_2 and not proportional to $(1 - (L_1/L_2)^2)^{1/2}$.

in the direction of increasing r as F_{ef} . F_{ef} is given by

$$F_{ef} = T \frac{\partial S_{AB}}{\partial r}, \quad (109)$$

where T is the temperature of the field of the outside region. To estimate F_{ef} , we set S_{AB} to that in Minkowski spacetime and T to the Hawking temperature $T = (8\pi G_N M)^{-1} = (4\pi R)^{-1}$. In this approximation the entropic force is *repulsion force* because S_{AB} increases when r increases. $\partial S_{AB}/\partial r$ is independent of the ultraviolet cutoff, and then we obtain

$$F_{ef} = -\frac{T}{R} S'_{A;B}(r/R) = -\frac{1}{4\pi R^2} S'_{A;B}(r/R), \quad (110)$$

where $S_{A;B} = S_A(R) + S_B(R) - S_{AB}(r, R)$ and $S'_{A;B} \equiv \partial S_{A;B}/\partial(r/R)$. ($S_{A;B}$ is independent of the ultraviolet cutoff and a function of r/R .) Then the ratio of the entropic force to the

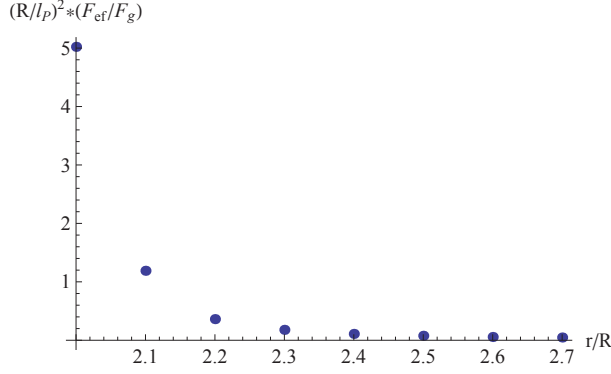


FIG. 18. The ratio of the entropic force to the force of gravity $\left(\frac{R}{l_P}\right)^2 \left|\frac{F_{ef}}{F_g}\right|$ as a function of r/R for $R/a = 10$.

force of gravity ($F_g = -\frac{G_N M^2}{r^2} = -\frac{R^2}{4G_N r^2}$) is

$$\left|\frac{F_{ef}}{F_g}\right| = \frac{1}{\pi} \left(\frac{l_P}{R}\right)^2 \left|\frac{S'_{A;B}(r/R)}{R^2/r^2}\right|, \quad (111)$$

where l_P is the Planck length $l_P = (G_N \hbar / c^3)^{1/2}$. When $r \gg R$, we substitute (107) into (111), and then we obtain

$$\left|\frac{F_{ef}}{F_g}\right| \approx 0.33 \left(\frac{l_P}{R}\right)^2 \frac{R^3}{r^3}. \quad (112)$$

When $r \approx R$, we show the computed values of $\left(\frac{R}{l_P}\right)^2 \left|\frac{F_{ef}}{F_g}\right|$ as a function of r/R for $R/a = 10$ in Fig.18. (Although from (111) $\left(\frac{R}{l_P}\right)^2 \left|\frac{F_{ef}}{F_g}\right|$ is a function of r/R and is independent of the choice of the value of R/a , the computed values of $\left(\frac{R}{l_P}\right)^2 \left|\frac{F_{ef}}{F_g}\right|$ slightly depend on the choice of the value of R/a because the spheres on the lattice are distorted. When R/a is large, the spheres on the lattice are similar to the real spheres and this R/a dependence is small.) From (112) and Fig.18 the entropic force is much smaller than the force of gravity when $R \gg l_P$ and comparable to the force of gravity when $R \approx l_P$.

X. CONCLUSIONS AND DISCUSSION

In Section III we showed that the entanglement entropy ($S_C = S_{AB}$) of two disjoint regions in translational invariant vacuum in general QFT reaches its maximum value when $r \rightarrow \infty$. And we obtained the inequality (9). In Section V we developed the method to obtain the r dependence of S_C and obtained the r dependence of S_C (68) in the free massless scalar field

in $(d + 1)$ dimensional Minkowski spacetime. We can use this method in curved space time and for scalar field theory whose Lagrangian is quadratic. To know only the r dependence we need only the $\|x - y\|$ dependence of $W(x, y)$ and $W^{-1}(x, y)$ when $\|x - y\|$ is large. To know the R_1 and R_2 dependence we must solve the zeroth order eigenvalue equation and obtain λ_m^0 and $f_{mi\alpha}^0$. It is difficult to solve the zeroth order eigenvalue equation analytically, so we need to perform numerical calculation. But we assumed the $R \equiv R_1 = R_2$ dependence (70) by using dimensional analysis and the cutoff dependence of S_A and S_B .

In Section VI we showed that S_C can be expected to be the form (78) in the black hole case. In this case the only assumption we made is the r dependence of $W(x_a, y_b)$ and $W^{-1}(x_a, y_b)$. We did not explicitly calculate $W(x_a, y_b)$ and $W^{-1}(x_a, y_b)$, but assumed the r dependence of $W(x_a, y_b)$ and $W^{-1}(x_a, y_b)$ by dimensional analysis.

In Section VII we assumed that we can consider the entanglement entropy of two black holes as thermodynamic entropy, and investigated its entropic force. We considered three situations (1), (2) and (3) and obtain the relationship (88) between the force acting on one black hole or on one ball and the sum of the Casimir force and the effect of the entanglement entropic force. Because we can probably neglect the Casimir force, we can confirm (88) experimentally in principle.

Next we discuss the entanglement entropic force in different systems. In the black hole case, black holes act as *"walls" which hide inside regions but hold the entanglement between inside and outside regions*. So if there are walls of this type, the entanglement entropic force will exist between regions surrounded by these walls. Then we will be able to confirm the entanglement entropic force by experiments in a laboratory if we make this wall. And if entanglement entropy depends on some external parameter, entanglement entropic force probably appears also in quantum mechanical (i.e. not quantum field theoretical) systems.

In Section VIII and IX we calculated numerically the entanglement entropy S_{AB} of two spheres and obtained the approximate expression (107). From Fig.12, (107) is precise for relatively small r . (When $R_1 = R_2 \equiv R$, for $r \gtrsim 3R$ (107) is precise from Fig.12.) We showed that the mutual information $S_{A;B}$ of A and B is independent of the ultraviolet cutoff for $d = 2, 3$ though S_A and S_B depends on the ultraviolet cutoff. The mutual information $S_{A;B}$ measures the entanglement between A and B and S_A measures the entanglement between A and A^c where A^c is the complementary of A . Then our results mean that the ultraviolet divergence of entanglement entropy in QFT is caused by the entanglement between points

which are infinitely close to each other and the entanglement between regions which are finitely separate from each other is finite. And we showed that $S_{A;B}$ is the simple product of a function of R_1 and that of R_2 for $d = 2, 3$. These properties of $S_{A;B}$ for $d = 2, 3$ are most likely the same as those for $d \geq 4$. Then, from (1), for $d \geq 4$ when $r \gg R_1, R_2$ we assume

$$S_{A;B} \approx \frac{g_d R_1^{d-1} R_2^{d-1}}{r^{2d-2}}, \quad (113)$$

where $g_d \geq 0$ is a dimensionless constant.

In order to examine whether only the degrees of freedom on the surface of the spheres contribute to the mutual information or not, we calculate the mutual information $S_{D;E}$ of two same spherical shells D and E for $d = 3$ and the mutual information $S_{H;I}$ of two same rings H and I for $d = 2$. We obtained the result that not only the degrees of freedom on the surface of the sphere but also those on the inside region contribute to the mutual information, and the degrees of freedom on the inside region does not contribute uniformly to the mutual information. Because $S_{D;E}$ and $S_{H;I}$ measure the entanglement between regions which are finitely separate from each other, it is natural that the inside region contribute to the mutual information. The result that the inside region does not contribute uniformly to the mutual information means that the mutual information is not the product of the simple sum of the contribution from each volume elements. These results are different from that of the entanglement entropy to which the degrees of freedom on the surface of the boundary contribute mainly and uniformly. So the mutual information of two disconnected regions is not universally proportional to the product of the surface areas of the regions. Because a sphere has only one dimensionful parameter, the mutual information of two spheres is proportional to the product of the surface areas. For example, the mutual information of two rectangular solids is most likely not proportional to the product of the surface areas because a rectangular solid has three dimensionful parameters.

Our numerical method has three properties. First, we take the volume of the whole space to infinity, i.e. $N \rightarrow \infty$ in (94) and (95). Second, the computational complexity of our method depends only on the number of points on the regions of which we compute the entanglement entropy and does not depend on the distance between the separated regions. The computational complexity of conventional methods increases when the distance between the separated regions increases. This is because the numerical integrals of W_{mn} in (98) and W_{mn}^{-1} in (99) converge very slowly when $\|n - m\| \gg 1$. In order to reduce the computational

complexity of W_{mn} and W_{mn}^{-1} , we use the approximate expressions (101) and (103) when $\|n - m\| > 10$. Third, we can compute the entanglement entropy of general shaped regions by our method because we do not use any symmetry of the regions of which we compute the entanglement entropy in our method. For example, we can compute the entanglement entropy of more than two separated regions. The first and the second properties enable us to obtain the r dependence of S_{AB} . And the third property enable us to compute S_{AB} for $R_1 \neq R_2$.

We estimated roughly the magnitude of the entropic force between two black holes. From (112) and Fig.18 the entropic force is comparable to the force of gravity when $R \approx l_P$. This rough estimate suggests that the entropic force is important for Planck scale black holes. (Of course, this result would be changed if the effect of quantum gravity would be taken into account when $R \approx l_P$.)

Next, we discuss the microscopic origin of the entropic force. As we see from (110) the entropic force is proportional to the r derivative of the mutual information $S_{A;B}$. So the origin of the entropic force is the entanglement between inside regions of two black holes. Due to the entanglement between inside regions of two black holes, the density matrix of the scalar field on the outside region changes when r changes. Then the force acts on black holes along the direction in which S_{AB} increases.

Finally we mention the validity of this estimate. When $r \gg R$, it is shown that $S_{A;B}$ in the black holes case can be expected to be similar to that in the Minkowski spacetime case except for the coefficient because almost all regions between two black holes is similar to Minkowski spacetime [12]. So, the rough estimate corresponds to the contribution to F_{ef} in (109) from $S_{A;B}$. However, in the black holes case S_A and S_B depend on r and contribute to F_{ef} . These contribution from S_A and S_B has been discussed in [12]. When $r \approx R$, $S_{A;B}$ in the black holes case is probably different from that in the Minkowski spacetime case because the region between two black holes is very different from Minkowski spacetime. However, even when $r \approx R$, $S_{A;B}$ is most likely independent of the ultraviolet cutoff as that in the Minkowski spacetime case.

ACKNOWLEDGMENTS

I am grateful to Takahiro Kubota, Yutaka Hosotani and Satoshi Yamaguchi for teaching me various things and continuous encouragements. I also would like to thank Kin-ya Oda, Kunio Kaneta, Ryoutaro Watanabe, Tadashi Okazaki, Takuya Shimotani, Akinori Tanaka and all the other members of particle physics theory group at Osaka University for many stimulating discussions and encouragements.

Appendix A: The calculation of W and W^{-1}

In this appendix we calculate $W(x, y)$ and $W^{-1}(x, y)$ ((25) and (26)) explicitly. We regularize them by including convergence factor $e^{-l|k|}$ in them, where l is the cutoff length. We define W_α as

$$W_\alpha(x, y) = \int \frac{d^d k}{(2\pi)^d} (k^2)^{(1-\alpha)/2} e^{ik \cdot (x-y)} e^{-l|k|}. \quad (\text{A1})$$

Then we have $W_0 = W$ and $W_2 = W^{-1}$. First we consider the case $d \geq 3$.

(1) $d \geq 3$

We perform the integrals of angular coordinates which do not enter the inner product,

$$W_\alpha(x, y) = \frac{1}{(2\pi)^d} \prod_{m=2}^{d-2} \left(\sqrt{\pi} \frac{\Gamma\left(\frac{d-m}{2}\right)}{\Gamma\left(\frac{d-m+1}{2}\right)} \right) \int_0^\infty dk \int_{-1}^1 dt [1-t^2]^{\frac{d-3}{2}} e^{ikrt} e^{-lk} k^{d-\alpha} \quad (\text{A2})$$

where $r \equiv \|x - y\|$ and we change the variable as $t = \cos \theta$. Next we perform the k integral

$$\begin{aligned} \int_0^\infty dk \int_{-1}^1 dt [1-t^2]^{\frac{d-3}{2}} e^{ikrt} e^{-lk} k^{d-\alpha} &= \int_{-1}^1 dt [1-t^2]^{\frac{d-3}{2}} \left(\frac{1}{it} \frac{d}{dr} \right)^{d-\alpha} \int_0^\infty dk e^{ikrt} e^{-lk} \\ &= (-i)^{d-\alpha-1} (d-\alpha)! \frac{1}{r^{d-\alpha+1}} \int_{-1}^1 dt [1-t^2]^{\frac{d-3}{2}} \frac{1}{(t+iz)^{d-\alpha+1}} \end{aligned} \quad (\text{A3})$$

where $z \equiv l/r$. We define

$$g(t) \equiv [1-t^2]^{\frac{d-3}{2}} \frac{1}{(t+iz)^{d-\alpha+1}}. \quad (\text{A4})$$

We want to show $W_\alpha \neq 0$ when $z \rightarrow 0$.

(i) $d = 2m + 2$ ($m \geq 1$)

In this case $g(t)$ has a branch cut on the real axis from -1 to 1 . We perform the integration along the contour shown in Fig 19 (a), and obtain

$$\int_{-1}^1 dt g(t) = \pi i \text{Res}_{t=-iz} g(t) = \pi i \frac{1}{(d-\alpha)!} \left(\frac{d^{d-\alpha}}{dt^{d-\alpha}} [1-t^2]^{\frac{d-3}{2}} \right) \Big|_{t=-iz}. \quad (\text{A5})$$

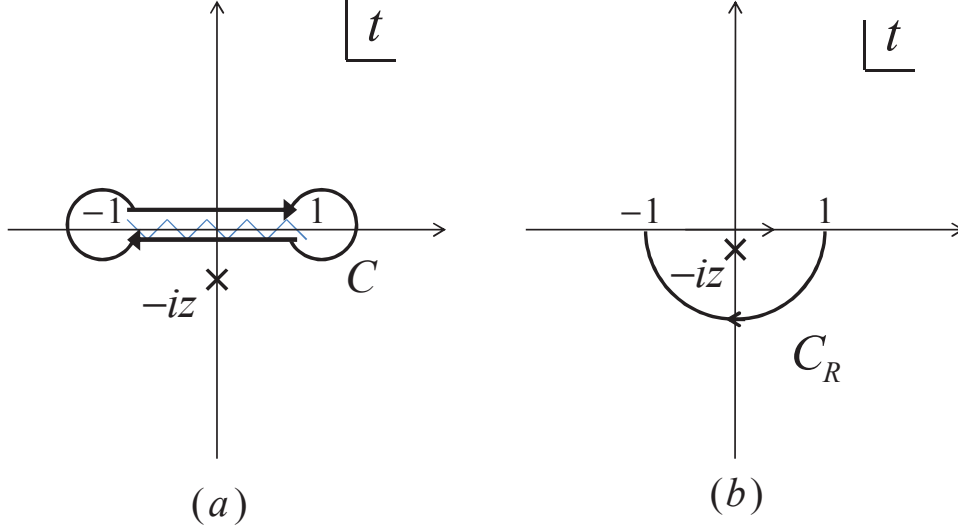


FIG. 19. The contours of the integrals. (a) $d = 2m + 2$ ($m \geq 1$). (b) $d = 2m + 1$ ($m \geq 1$).

The derivative in (A5) can be calculated by the derivative of a composite function,

$$\left(\frac{d^{d-\alpha}}{dt^{d-\alpha}} [1-t^2]^{\frac{d-3}{2}} \right) = \sum_{r=0}^{\lfloor \frac{1}{2}(d-\alpha) \rfloor} \frac{(d-\alpha)!}{r!(d-\alpha-2r)!} (2t)^{d-\alpha-2r} (-1)^{d-\alpha-r} \left(\frac{d-3}{2} \right) \left(\frac{d-3}{2} - 1 \right) \cdots \left(\frac{d-3}{2} - (d-\alpha-r-1) \right) (1-t^2)^{\frac{d-3}{2} - (d-\alpha-r)}$$
(A6)

where $\lfloor \frac{1}{2}(d-\alpha) \rfloor$ is the Gauss' symbol which is the greatest integer that is less than or equal to $\frac{1}{2}(d-\alpha)$.

Then, when $z \rightarrow 0$, we obtain

$$\begin{aligned} \int_{-1}^1 dtg(t) &= -\pi i \frac{1}{\left(\frac{d-\alpha}{2}\right)!} (-1)^{\frac{d-\alpha}{2}} \left(\frac{d-3}{2}\right) \left(\frac{d-3}{2} - 1\right) \cdots \left(\frac{d-3}{2} - \left(\frac{d-\alpha}{2} - 1\right)\right) \\ &= -\pi i \frac{1}{\left(\frac{d-\alpha}{2}\right)!} \left(-\frac{1}{2}\right)^{\frac{d-\alpha}{2}} (d-3)(d-1) \cdots (\alpha-1). \end{aligned}$$
(A7)

Then, from (A2), (A3) and (A7), for $\alpha = 2l \leq d$ ($l \in \mathbb{Z}$) W_α is nonzero and W_α has the form of (29) when $z \rightarrow 0$. (When $\alpha = d$, we obtain $\int_{-1}^1 dtg(t) = -\pi i$ from (A5). (Note that $g(t)$ has the branch cut, then $[1+z^2]^{(d-3)/2} \rightarrow (-1)$ when $z \rightarrow 0$.)

(ii) $d = 2m + 1$ ($m \geq 1$)

We perform the integration along the contour shown in Fig 19 (b), and obtain

$$\int_{-1}^1 dtg(t) = -2\pi i \text{Res}_{t=-iz} g(t) - \int_{C_R} dtg(t).$$
(A8)

For $\alpha = 2l (l \in \mathbb{Z})$, $d - \alpha$ is odd, so we obtain $\lim_{z \rightarrow 0} \text{Res}_{t=-iz} g(t) = 0$ from (A6). Then, for $\alpha = 2l$ and $z \rightarrow 0$ we obtain

$$\begin{aligned}
\int_{-1}^1 dtg(t) &= - \int_{C_R} dtg(t) = i(-1)^{d-\alpha} \int_0^\pi d\theta e^{-i(d-\alpha)\theta} [1 - e^{2i\theta}]^{\frac{d-3}{2}} \\
&= i(-1)^{d-\alpha} (-2i)^{m-1} \int_0^\pi d\theta e^{-i(2m+1-\alpha)\theta} e^{i(m-1)\theta} (\sin \theta)^{m-1} \\
&= (-1)^m 2^{2m-1} i^m (I_{sc}[m-1, m+2-\alpha] - iI_{ss}[m-1, m+2-\alpha]) \\
&= \begin{cases} 2^{m-1} i^{m+1} I_{ss}[m-1, m+2-\alpha] \neq 0 & \text{for odd } m, \\ 2^{m-1} i^m I_{sc}[m-1, m+2-\alpha] \neq 0 & \text{for even } m, \end{cases} \tag{A9}
\end{aligned}$$

where

$$I_{sc}[m, n] \equiv \int_0^\pi d\theta (\sin \theta)^m \cos(n\theta), \quad I_{ss}[m, n] \equiv \int_0^\pi d\theta (\sin \theta)^m \sin(n\theta). \tag{A10}$$

Then, from (A2) (A7) and (A9), for $\alpha = 2l (l \in \mathbb{Z})$ W_α is nonzero and W_α has the form of (29) when $z \rightarrow 0$.

From (i) and (ii) we showed (29) for $d \geq 3$. Next we consider $d = 2$.

(2) $d = 2$

In this case we can perform the angular integral first,

$$\begin{aligned}
W_\alpha(x, y) &= \frac{1}{(2\pi)^2} \int_0^\infty k dk \int_0^{2\pi} d\theta k^{1-\alpha} e^{ikr \cos \theta - lk} \\
&= \frac{1}{2\pi} \int_0^\infty dk k^{2-\alpha} e^{-lk} J_0(kr) = \frac{1}{2\pi r^{3-\alpha}} \int_0^\infty dx x^{2-\alpha} e^{-zx} J_0(x)
\end{aligned} \tag{A11}$$

where J_0 is the Bessel function of zeroth order. We perform the integral for $\alpha = 2$ and $\alpha = 0$.

(i) $\alpha = 2$

In this case we have

$$\int_0^\infty dx e^{-zx} J_0(x) = \frac{1}{\sqrt{z^2 + 1}}. \tag{A12}$$

Then, when $z \rightarrow 0$ we obtain

$$W_{\alpha=2}(x, y) = W^{-1}(x, y) = \frac{1}{2\pi r}. \tag{A13}$$

(i) $\alpha = 0$

In this case we have

$$\int_0^\infty dx x^2 e^{-zx} J_0(x) = \frac{\Gamma(3)}{z^3} F\left(\frac{3}{2}, 2, 1; -\frac{1}{z^2}\right) \rightarrow -1 \quad (z \rightarrow 0) \tag{A14}$$

where F is the Gaussian hypergeometric function. Then, when $z \rightarrow 0$ we obtain

$$W_{\alpha=0}(x, y) = W(x, y) = \frac{-1}{2\pi r^3}. \quad (\text{A15})$$

Finally we have showed (29) for $d \geq 2$.

Appendix B: A formula for a finite series

In this appendix we obtain a formula for a finite series by calculating the following integral.

$$A \equiv \int_0^\infty dk k^{2c} \int_0^\pi d\theta (\sin \theta)^{2b} e^{ikr \cos \theta - \epsilon k} \quad c \geq b \geq 0 \quad b, c \in \mathbb{Z} \quad \epsilon, r > 0 \quad \epsilon, r \in \mathbb{R}. \quad (\text{B1})$$

This integral is a generalization of W_α in (A1). The parameter ϵ and r are auxiliary and they do not appear in the last formula. We obtain the finite series when we perform the θ integral before performing the k integral. On the other hand we obtain the simple expression when we perform the k integral before performing the θ integral. Then we obtain the formula for the finite series.

(i) We perform the θ integral before performing the k integral.

We perform the θ integral,

$$\int_0^\pi d\theta (\sin \theta)^{2b} e^{ikr \cos \theta} = \left(1 + \frac{1}{k^2} \frac{d^2}{dr^2}\right)^b \int_0^\pi d\theta e^{ikr \cos \theta} = \pi \left(1 + \frac{1}{k^2} \frac{d^2}{dr^2}\right)^b J_0(kr) \quad (\text{B2})$$

where J_0 is the Bessel function of zeroth order. We substitute (B2) into (B1) and perform the k integral. Then we obtain

$$A = \pi \sum_{l=0}^b {}_bC_l \left(\frac{d}{dr}\right)^{2l} \int_0^\infty dk e^{-\epsilon k} k^{a-2l} J_0(kr) = \pi \sum_{l=0}^b {}_bC_l \left(\frac{d}{dr}\right)^{2l} \frac{\Gamma(\mu)}{\epsilon^\mu} F\left(\frac{\mu}{2}, \frac{\mu+1}{2}, 1; -\frac{r^2}{\epsilon^2}\right) \quad (\text{B3})$$

where $\mu \equiv 2c - 2l + 1$ and F is the Gaussian hypergeometric function. We have used the condition $c \geq b \geq 0$ in the second equality in (B3). When $\epsilon \rightarrow 0$, we obtain

$$\lim_{\epsilon \rightarrow 0} \frac{\Gamma(\mu)}{\epsilon^\mu} F\left(\frac{\mu}{2}, \frac{\mu+1}{2}, 1; -\frac{r^2}{\epsilon^2}\right) = \frac{\pi^{1/2}}{r^\mu} \frac{\Gamma(\mu)}{\Gamma(1 - \frac{\mu}{2})\Gamma(\frac{1+\mu}{2})}. \quad (\text{B4})$$

From (B3) and (B4) we obtain

$$\lim_{\epsilon \rightarrow 0} A = \pi^{3/2} \sum_{l=0}^b {}_bC_l \frac{\Gamma(\mu)}{\Gamma(1 - \frac{\mu}{2})\Gamma(\frac{1+\mu}{2})} \left(\frac{d}{dr}\right)^{2l} \frac{1}{r^\mu} = \frac{\pi^{3/2}}{r^{2c+1}} (2c)! \sum_{l=0}^b {}_bC_l \frac{1}{\Gamma(1 - \frac{\mu}{2})\Gamma(\frac{1+\mu}{2})}. \quad (\text{B5})$$

(ii) We perform the k integral before performing the θ integral.

We change the variable as $t = \cos \theta$ and perform the k integral,

$$\begin{aligned}
A &= \int_{-1}^1 dt [1 - t^2]^{b-1/2} \int_0^\infty dk k^{2c} e^{ikrt - \epsilon k} = \int_{-1}^1 dt [1 - t^2]^{b-1/2} \left(\frac{1}{it} \frac{d}{dr} \right)^{2c} \int_0^\infty dk e^{ikrt - \epsilon k} \\
&= i^{2c+1} \frac{(2c)!}{r^{2c+1}} \int_{-1}^1 dt [1 - t^2]^{b-1/2} \frac{1}{(t + iz)^{2c+1}}
\end{aligned} \tag{B6}$$

where $z \equiv \epsilon/r$. We perform the integration along the contour shown in Fig 19 (a) in the same way as Eqs.(A5)-(A7), and obtain

$$\begin{aligned}
\lim_{\epsilon \rightarrow 0} A &= i^{2c+1} \frac{(2c)!}{r^{2c+1}} (-i\pi) \frac{1}{c!} (-1)^c (b - \frac{1}{2})(b - \frac{3}{2}) \dots (b - c + \frac{1}{2}) \\
&= \pi \frac{(2c)!}{r^{2c+1} c!} (b - \frac{1}{2})(b - \frac{3}{2}) \dots (b - c + \frac{1}{2}) \\
&= \pi \frac{(2c)!}{r^{2c+1} c!} \frac{(-1)^{c-b}}{2^c} (2b - 1)!! (2c - 2b - 1)!!
\end{aligned} \tag{B7}$$

From (B5) = (B7) we obtain the formula for the finite series. We simplify (B5) = (B7) and obtain the following formula,

$$\sum_{l=0}^b (-2)^l \frac{(2c - 2l - 1)!!}{l!(b-l)!(c-l)!} = (-1)^b \frac{(2b - 1)!! (2c - 2b - 1)!!}{b! c!} \quad c \geq b \geq 0 \quad b, c \in \mathbb{Z}. \tag{B8}$$

We can also rewrite (B8) as follows;

$$\sum_{l=0}^b (-4)^l \frac{(2c - 2l)!}{l!(b-l)![(c-l)!]^2} = (-1)^b \frac{(2b)!(2c - 2b)!}{(b!)^2 c! (c - b)!} \quad c \geq b \geq 0 \quad b, c \in \mathbb{Z}. \tag{B9}$$

- [1] L. Bombelli, R. K. Koul, J. Lee, and R. D. Sorkin, Phys. Rev. D34, 373 (1986)
- [2] M. Srednicki, Phys. Rev. Lett. 71, 666 (1993), arXiv:hep-th/9303048
- [3] S. Hawking, J. M. Maldacena, and A. Strominger, JHEP 05, 001 (2001), arXiv:hep-th/0002145
- [4] D. N. Kabat, Nucl. Phys. B453, 281 (1995), arXiv:hep-th/9503016
- [5] L. Susskind and J. Uglum, Phys. Rev. D50, 2700 (1994), arXiv:hep-th/9401070
- [6] V. P. Frolov and I. Novikov, Phys. Rev. D48, 4545 (1993), arXiv:gr-qc/9309001
- [7] T. Jacobson, (1994), arXiv:gr-qc/9404039
- [8] G. 't Hooft, Nucl. Phys. B256, 727 (1985)

- [9] H. Casini and M. Huerta, JHEP 0903, 048 (2009), arXiv:0812.1773 [hep-th].
- [10] P. Calabrese, J. Cardy, and E. Tonni, J.Stat.Mech. 0911, P11001 (2009), arXiv:0905.2069 [hep-th].
- [11] P. Calabrese, J. Cardy, and E. Tonni, J.Stat.Mech. 1101, P01021 (2011), arXiv:1011.5482 [hep-th].
- [12] N. Shiba, Phys.Rev. D83, 065002 (2011), arXiv:1011.3760 [hep-th].
- [13] N. Shiba, JHEP 07, 100 (2012), arXiv:1201.4865 [hep-th] .
- [14] M. Nielsen and I. Chuang, *Quantum Computation and Quantum Information* (Cambridge University Press, Cambridge, England, 2000), p. 9.
- [15] P. Calabrese and J. L. Cardy, J. Stat. Mech. 0406, P002 (2004), arXiv:hep-th/0405152
- [16] C. Holzhey, F. Larsen, and F. Wilczek, Nucl. Phys. B424, 443 (1994), arXiv:hep-th/9403108
- [17] S. Ryu and T. Takayanagi, Phys. Rev. Lett. 96, 181602 (2006), arXiv:hep-th/0603001
- [18] S. Ryu and T. Takayanagi, JHEP 08, 045 (2006), arXiv:hep-th/0605073
- [19] H. Casini and M. Huerta, J. Phys. A42, 504007 (2009), arXiv:0905.2562 [hep-th]
- [20] S. N. Solodukhin, Living Rev.Rel. 14, 8 (2011), arXiv:1104.3712 [hep-th].
- [21] M. Creutz, *Quarks, gluons and lattices* (Cambridge Univ Pr, 1985).
- [22] T. Emig, N. Graham, R. L. Jaffe, and M. Kardar, Phys. Rev. Lett. 99, 170403 (2007), arXiv:0707.1862 [cond-mat.stat-mech]
- [23] J. Cardy, J.Phys. A46, 285402 (2013), arXiv:1304.7985 [hep-th] .
- [24] T. Takayanagi, private communication.
- [25] When $d=1$, this is not correct because generally the correlation function $\langle 0 | \phi(t, x) \phi(t, y) | 0 \rangle$ does not become zero when $|x - y| \rightarrow \infty$. For example the correlation function of massless free scalar fields does not become zero when $|x - y| \rightarrow \infty$.
- [26] We use the following easily verifiable identity,

$$\begin{pmatrix} A & C \\ D & B \end{pmatrix} = \begin{pmatrix} A - CB^{-1}D & CB^{-1} \\ 0 & 1 \end{pmatrix} \begin{pmatrix} 1 & 0 \\ D & B \end{pmatrix} = \begin{pmatrix} A & 0 \\ D & 1 \end{pmatrix} \begin{pmatrix} 1 & A^{-1}C \\ 0 & B - DA^{-1}C \end{pmatrix}.$$